ALZHEIMER'S DISEASE

# Aβ and tau prion-like activities decline with longevity in the Alzheimer's disease human brain



Atsushi Aoyagi[1,2]*, Carlo Condello[1,3]*†, Jan Stöhr[1,3,4], Weizhou Yue[1], Brianna M. Rivera[1], Joanne C. Lee[1], Amanda L. Woerman[1,3], Glenda Halliday[5], Sjoerd van Duinen[6], Martin Ingelsson[7], Lars Lannfelt[7], Caroline Graff[8,9], Thomas D. Bird[10,11], C. Dirk Keene[12], William W. Seeley[3,13], William F. DeGrado[1,14], Stanley B. Prusiner[1,3,15]†

**The hallmarks of Alzheimer's disease (AD) are the accumulation of Aβ plaques and neurofibrillary tangles composed of hyperphosphorylated tau. We developed sensitive cellular assays using human embryonic kidney–293T cells to quantify intracellular self-propagating conformers of Aβ in brain samples from patients with AD or other neurodegenerative diseases. Postmortem brain tissue from patients with AD had measurable amounts of pathological Aβ conformers. Individuals over 80 years of age had the lowest amounts of prion-like Aβ and phosphorylated tau. Unexpectedly, the longevity-dependent decrease in self-propagating tau conformers occurred in spite of increasing amounts of total insoluble tau. When corrected for the abundance of insoluble tau, the ability of postmortem AD brain homogenates to induce misfolded tau in the cellular assays showed an exponential decrease with longevity, with a half-life of about one decade over the age range of 37 to 99 years. Thus, our findings demonstrate an inverse correlation between longevity in patients with AD and the abundance of pathological tau conformers. Our cellular assays can be applied to patient selection for clinical studies and the development of new drugs and diagnostics for AD.**

## INTRODUCTION

The plaques and tangles of Alzheimer's disease (AD) were first described more than a century ago (*1*). In 1984, the amyloid-β (Aβ) peptide was described (*2*), and the tau protein in neurofibrillary tangles (NFTs) was reported soon thereafter (*3*–*6*). Both Aβ and tau proteins adopt pathogenic conformations that spread through the brain (*7*, *8*) in a manner similar to the prion protein ($PrP^{Sc}$), which causes Creutzfeldt-Jakob disease, Gerstmann-Sträussler-Scheinker (GSS) disease, fatal familial insomnia, and kuru (*9*). Because our knowledge of prions has expanded with the identification of physiological nonpathogenic prions, a more inclusive definition has emerged: Prions are composed of host-encoded proteins that adopt alternative conformations, which are self-propagating (*10*). Here, we refer to Aβ and tau as "prion-like" proteins.

Although the vast majority of AD cases are sporadic, an important but small number of familial cases have been instructive. In 1989, one of us reported genetic linkage of the P102L mutation in the PrP open reading frame that causes familial GSS (*11*). Two years later, familial AD was linked to the V717I mutation in the amyloid precursor protein (APP) open reading frame (*12*). The importance of Aβ was further elucidated through investigations of AD pathogenesis based on genetic linkage studies between inherited AD and mutations in either APP or its processing enzymes (*13*, *14*). Sequential cleavage of APP yields Aβ40 and Aβ42 as the major peptide isoforms (*14*). Aβ42 can polymerize into oligomers or fibrils and ultimately forms amyloid deposits in the brain (*14*). The role of tau in AD was clarified in 1998 when three different point mutations in the *MAPT* gene encoding tau protein isoforms were shown to cause familial Pick's disease (*15*, *16*).

In familial cases of cerebral amyloid angiopathy (CAA) caused by mutations in the Aβ coding region of APP, death generally occurs in the fourth or fifth decade of life and in the absence of substantial accumulation of insoluble tau (*17*, *18*). In contrast to CAA, misfolded tau spreads through many brain regions in both sporadic and familial AD, resulting in cognitive decline. Hypotheses about the role of Aβ abound: Aβ deposition is considered inconsequential by some (*19*, *20*), or Aβ is thought to transiently initiate tau misfolding and polymerization into NFTs by others (*21*–*24*). Aβ might also have transient toxicity due to the accumulation of Aβ oligomers, which peak in the early, prodromal phase of AD progression (*25*, *26*). Alternatively, an early steady progression of Aβ oligomerization, deposition, and spreading has been proposed. The latter hypothesis is supported by the correlation of increasing AD severity with the spread of Aβ throughout the brain (*27*, *28*) and decreased Aβ42 in cerebrospinal fluid (CSF) (*29*). In this view, early and progressive formation of prion-like Aβ conformers leads to dysfunction in the central nervous system (CNS), including an inability to clear misfolded tau molecules leading to the accumulations of NFTs.

To address this hypothesis, assays are needed to measure and rapidly compare Aβ and tau prion-like activities in the postmortem

[1]Institute for Neurodegenerative Diseases, UCSF Weill Institute for Neurosciences, University of California, San Francisco, San Francisco, CA 94158, USA. [2]Daiichi Sankyo Co. Ltd., Tokyo 140-8710, Japan. [3]Department of Neurology, UCSF Weill Institute for Neurosciences, University of California, San Francisco, San Francisco, CA 94158, USA. [4]AC Immune SA, EPFL Innovation Park, Building B, 1015 Lausanne, Switzerland. [5]NeuRA and School of Medical Sciences, University of New South Wales, and Brain and Mind Centre, University of Sydney, Sydney, NSW 2052, Australia. [6]Leiden University Medical Center, Leiden, Netherlands. [7]Department of Public Health and Caring Sciences/Geriatrics, Uppsala University, 751 85 Uppsala, Sweden. [8]Department of Neurobiology, Care Sciences and Society, Karolinska Institute, Solna, Sweden. [9]Unit for Hereditary Dementias, Theme Aging, Karolinska University Hospital, Solna, Sweden. [10]Department of Medicine, Division of Medical Genetics, University of Washington, Seattle, WA 98195, USA. [11]Department of Neurology, University of Washington, Seattle, WA 98195, USA. [12]Department of Neuropathology, University of Washington School of Medicine, Seattle, WA 98195, USA. [13]Department of Pathology, University of California, San Francisco, San Francisco, CA 94143, USA. [14]Department of Pharmaceutical Chemistry, University of California, San Francisco, San Francisco, CA 94158, USA. [15]Department of Biochemistry and Biophysics, University of California, San Francisco, San Francisco, CA 94158, USA.
*These authors contributed equally to this work.
†Corresponding author. Email: carlo.condello@ucsf.edu (C.C.); stanley.prusiner@ucsf.edu (S.B.P.)

brain tissue of deceased patients with AD. However, current methods for the measurement of pathogenic Aβ conformations rely on either time-consuming transgenic mouse models or in vitro biophysical methods that are performed at superphysiological peptide concentrations. Earlier studies showed that AD patient brain–derived Aβ and synthetic Aβ injected into a transgenic mouse brain behaved in a prion-like manner (*30*–*34*). Current clinical imaging ligands measure insoluble amyloids, the role of which in disease is uncertain. These imaging methods fail to measure biologically active neuroinvasive prion-like Aβ and tau proteins. In contrast, highly reproducible and rapid cell-based methods have been devised to measure prion-like tau and α-synuclein proteins expressed as fusions with fluorescent proteins in mammalian cells (*35*–*38*). Here, we describe the development of an analogous cellular assay for Aβ, allowing Aβ and tau to be compared in postmortem brain tissue samples from patients with AD or other neurodegenerative diseases. Prion-like Aβ and tau activity decreased with longevity despite the presence of increasing NFTs. This decrease in tau prion-like activity paralleled similar decreases in tau phosphorylation. Thus, the greatest tau prion-like activities were found in individuals who died at relatively young ages, despite having the lowest abundance of total insoluble tau. It is the relative abundance of biologically active, phosphorylated prion-like tau and not the total amount of inert insoluble tau that correlated with longevity.

## RESULTS

### Development of isoform-specific and sequence-specific Aβ cellular assays

Following earlier studies (*39*–*41*), we built constructs in which Aβ40 and Aβ42 peptides were either N-terminally or C-terminally fused to yellow fluorescent protein (YFP) (Fig. 1A). Several structures of Aβ42 demonstrated that the C-terminal residues are buried in an inaccessible core (*42*–*44*), whereas the N terminus is largely disordered. We therefore compared constructs in which YFP was fused to either the N terminus or the C terminus of Aβ42. We then examined the ability of synthetic Aβ fibrils to induce aggregation of these constructs in the cytoplasm of mammalian human embryonic kidney–293T (HEK293T) cells, as determined from the number of cells showing yellow fluorescent puncta (Fig. 1, A to E). For these studies, we used a preparation of synthetic Aβ fibrils (fig. S1, A and B) that had previously been characterized biophysically and shown to act as prion-like particles as assessed from their ability to propagate their aberrant conformations after injection into the brains of transgenic mice (*33*, *34*). As expected, in our cellular assays, Aβ40 and Aβ42 fibrils were able to induce aggregation of YFP-Aβ42 fusion proteins in a dose-dependent manner, and this aggregation was most efficient when YFP was fused to the N terminus (Fig. 1D). We determined the fraction of cells that displayed punctate fluorescence due to the accumulation of aggregated YFP fusion proteins as a quantitative measure of prion-like activity. We designated the fraction of cells showing puncta as f(Aβ) (fraction of cells with puncta in which the particular protein fused to YFP is expressed and shown in parentheses). This cell line was designated YFP-Aβ42.

We also examined the formation of cytoplasmic puncta in an analogous cell line designated YFP-Aβ40, which expressed the Aβ40 rather than the Aβ42 isoform. Aβ40 fibrils—but not Aβ42 fibrils—were able to induce bright puncta in this YFP-Aβ40 cell line. Thus, in contrast to the YFP-Aβ42 cell line, the YFP-Aβ40 cell line was Aβ isoform specific (Fig. 1D and fig. S2A). We next introduced the familial mutations E22G, E22Q, and E22Δ into the YFP-Aβ40 cell lines (Fig. 1A). These cell lines showed high sensitivity for the formation of puncta when treated with wild-type (WT) Aβ40 fibrils, but not WT Aβ42 fibrils (Fig. 1E and fig. S2B). In contrast, synthetic WT Aβ40 fibrils were unable to induce f(Aβ) puncta in YFP-Aβ40 cells expressing the E22Δ mutation, a variant that is very prone to aggregation in vitro (*45*, *46*) (Fig. 1E and fig. S2B). These findings are similar to earlier biophysical studies measuring templating activities between WT Aβ and E22Δ Aβ (*47*). Thus, the YFP-Aβ40 cell line was useful for probing questions of isotype-specific induction of Aβ aggregation, whereas the YFP-Aβ42 cell line was more generally useful for measuring prion-like Aβ activity induced by exogenous addition of either Aβ40 or Aβ42 fibrils. Using the YFP-Aβ42 cell line, we determined quantitatively the prion-like Aβ titer from serial dilutions of various preparations ranging from synthetic peptide fibrils to human AD brain homogenates.

Next, we examined mouse brain–derived Aβ extracted using a sodium phosphotungstic acid (PTA) precipitation procedure (*48*). Aβ was extracted from the brains of transgenic mice (TgAPP23) expressing human mutant APP (*49*) that showed spontaneous Aβ deposition. The concentration of total Aβ determined by enzyme-linked immunosorbent assay (ELISA) that was required to stimulate intracellular f(Aβ) puncta formation in the YFP-Aβ42 cell line was about 10-fold lower than that for synthetic Aβ fibrils (Fig. 1C). We further defined the specificity of our bioassays using brain homogenates from transgenic mice carrying tau (*50*) or α-synuclein (*51*) mutations in the human *MAPT* or *SNCA* genes, respectively. These mice are commonly used to model the spontaneous accumulation of tau or α-synuclein aggregates in vivo. PTA-precipitated brain extracts from either mouse model did not stimulate f(Aβ) puncta formation in the YFP-Aβ42 cell line (Fig. 2, A and B). However, in cell lines expressing YFP fusions of the corresponding α-synuclein or tau mutant proteins, we observed intracellular prion-like activity of α-synuclein [f(syn)] or tau [f(tau)], respectively (Fig. 2, A and B).

### Increased prion-like Aβ titer, amyloid plaques, and gliosis in two transgenic mouse models of AD with age

We found previously (*32*) that formation of Aβ peptides increased with age and correlated with measures of neuroinflammation and pathology in two well-studied AD mouse models expressing human mutant transgenes: TgAPP23 and TgCRND8 (*49*, *52*). These two transgenic mouse strains exhibited progressive Aβ deposition with age (fig. S3, A and D) as well as glial inflammation, neuronal dysfunction, and cognitive deficits (*49*, *52*). To determine the progression of prion-like Aβ, we collected mouse brain samples over a ~2-year span in the slowly progressing TgAPP23 mouse model of AD. TgAPP23 mice display the first neuropathological brain changes between 6 and 9 months of age (*49*), with overt Aβ deposition appearing after ~1 year (390 days) (fig. S3A). Using our cellular assays, we found that the prion-like Aβ activity became detectable between 200 and 300 days of age, in parallel with the first appearance of amyloid plaques (fig. S3A) and astrocytic gliosis, which was measured using a bioluminescent reporter gene driven by the glial fibrillary acidic protein (GFAP) promoter (fig. S3B) (*32*). The number of f(Aβ) puncta measured using our HEK293T YFP-Aβ42 cell line continued to increase as the animals approached ~2 years of age (732 days) (fig. S3A). We observed similar results in the more rapidly progressing TgCRND8 mouse model of AD (fig. S3, D to F).

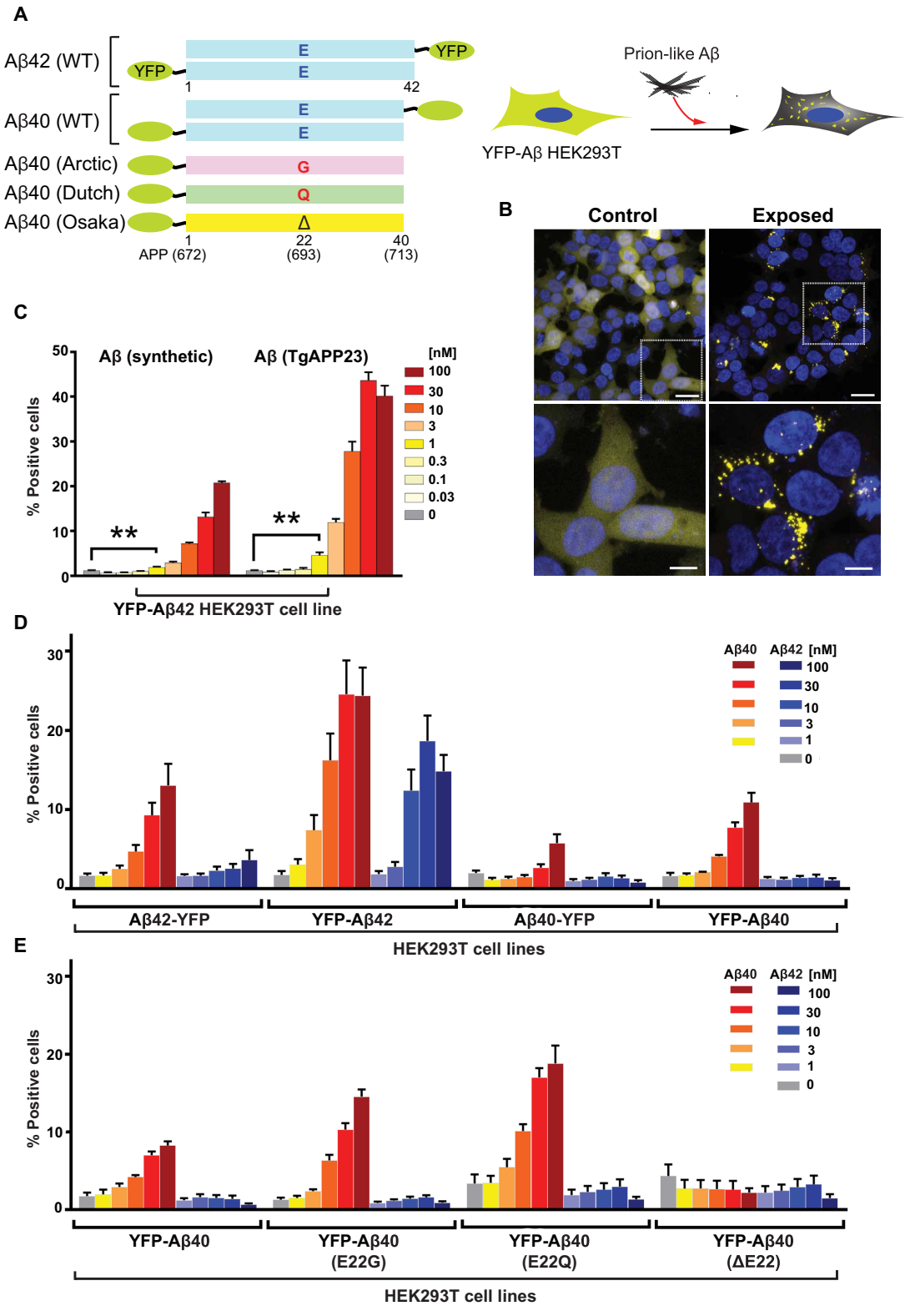


**Fig. 1. Development of YFP-Aβ fusion proteins in HEK293T cell lines for measuring Aβ aggregates in brain samples.** The indicated cell lines were developed to measure prion-like activity of preparations consisting of synthetic Aβ peptides and mouse brain–derived extracts based on their abilities to induce fluorescent aggregates (puncta). (**A**) Diagram illustrating the Aβ constructs used in this study (left). Stably transfected HEK293T cells expressing an Aβ-YFP fusion construct underwent Lipofectamine-based transduction with synthetic Aβ fibrils (right). (**B**) Representative confocal images of HEK293T cells expressing Aβ42 fused to YFP at the N terminus (clone #1), which were treated with phosphate-buffered saline (PBS) (left; control) or exposed to synthetic Aβ40 fibrils (initial monomeric concentration, 1 μM) (right, exposed). The aggregates of YFP-Aβ appear as fluorescent yellow puncta. To measure prion-like activity, we counted the number of puncta-positive cells and expressed this as a percent of the total number of cells in the field of view (% positive cells). Lower panels are higher-magnification images of white boxed areas in the upper panels. Scale bars, 20 μm (upper panels) or 5 μm (lower panels). (**C**) HEK293T cells transfected with YFP-Aβ42 were treated with two different types of Aβ ranging from 0.03 to 100 nM (initial monomeric concentration): synthetic Aβ40 (left) or Aβ purified from TgAPP23 mouse brains (right). Puncta-inducing activity in the HEK293T cells was quantified 2 days after the initial exposure to various Aβ preparations. Data shown are means ± SEM as determined from four images per well across four wells and are representative of three independent experiments. Statistical significance is indicated as $^{**}P < 0.01$. (**D**) Cell lines stably expressing four different WT Aβ constructs [shown in (A)] were developed, and puncta formation was compared with synthetic Aβ40 and Aβ42 isoforms. Quantification of Aβ in 16 monoclonal cell lines (four randomly chosen clones from each construct; see fig. S2A) was performed 2 days after exposure to increasing concentrations of synthetic Aβ40 or Aβ42 isoforms (1 to 100 nM) (see fig. S1). Data shown are means ± SEM as determined from four images per well across four wells and are representative of two to three independent experiments. (**E**) Cell lines stably expressing four different Aβ40 constructs fused to YFP at the N terminus [shown in (A)] were developed, and puncta formation was compared after exposure to synthetic Aβ40 and Aβ42 isoforms. Quantification of Aβ in 16 monoclonal cell lines (four randomly chosen clones from each construct; see fig. S2B) was performed 2 days after exposure to increasing concentrations of synthetic Aβ40 or Aβ42 isoforms (1 to 100 nM) (see fig. S1). Data shown are means ± SEM as determined from four images per well across four wells and are representative of two independent experiments.

### Human prion-like Aβ and tau accumulation as a function of age, gender, *APOE* ε4 genotype, and disease phenotype

Our Aβ cellular assays in combination with analogous tau cellular assays (*36*, *38*) enabled comparison of Aβ and tau prion-like activities in a collection of human postmortem brain tissue samples from patients with AD or other neurodegenerative diseases. We obtained postmortem human brain specimens from tissue banks (table S1) where the reported cause of death included a spectrum of neurodegenerative diseases ranging from "tau-only" dementias [e.g., frontotemporal lobar degeneration with tau-immunoreactive inclusions (FTLD-tau)] to Aβ-centric familial CAA. More specifically, in addition to 10 aged control brains from people who died of non-neurological diseases, we examined two types of FTLD-tau brain tissue samples from seven cases of progressive supranuclear palsy (PSP) and three cases of corticobasal degeneration (CBD). We also examined postmortem brain tissue from 37 patients with sporadic AD, 3 patients with sporadic CAA, and 47 patients with familial AD or familial CAA bearing disease-causing mutations in *APP*, *PSEN1*, or *PSEN2*. For each brain sample, we used PTA to selectively precipitate prion-like proteins from brain homogenates.

We next performed cellular assays for Aβ, tau, and α-synuclein using HEK293T cells expressing YFP-Aβ42, tau K18(LM)-YFP, or α-synuclein (A53T)-YFP, respectively (Fig. 3A). Elevated prion-like Aβ activities were detected in all of the AD and CAA brain samples (Fig. 3, C and D). In each brain tissue sample, the value of f(Aβ) was at least 20 SEs above the mean for the control brain samples, indicating that the prion-like Aβ puncta–inducing activity remained robust at the time of death in both AD and CAA and could be preserved by freezing. Additionally, all AD and CAA brain samples tested were devoid of puncta-inducing activity in the α-synuclein cellular assay, unlike postmortem brain samples from eight patients with MSA (Fig. 3E). Although tau puncta–inducing activity was detectable in all FTLD-tau brains, no measurable prion-like Aβ activity was found in these specimens (Fig. 3B), consistent with the classification of PSP and CBD as primary tauopathies.

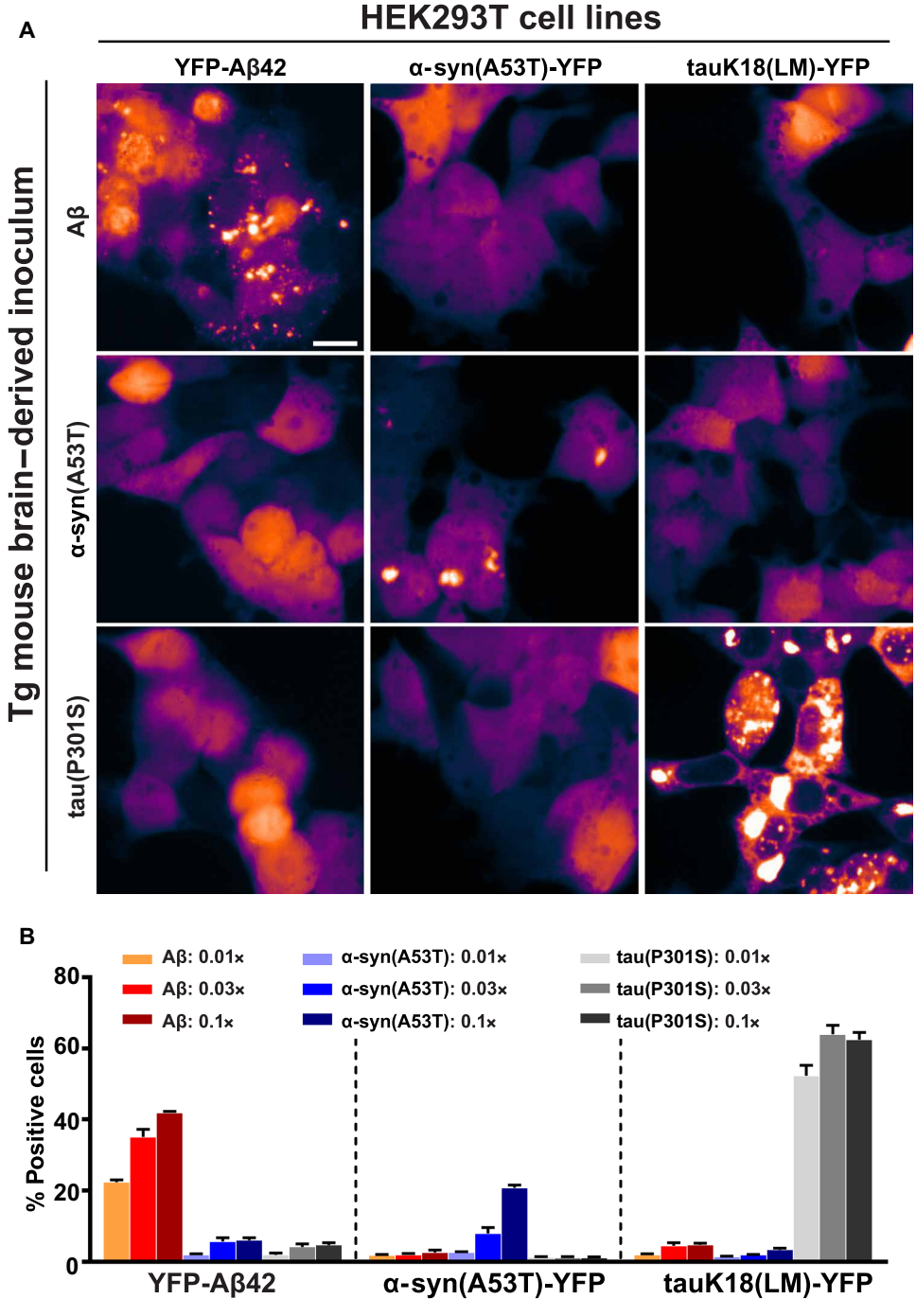


**Fig. 2. Specificity of the Aβ cellular assays.** Various transgenic mouse brain inocula were assayed for their Aβ, tau, and α-synuclein prion-like activities. (**A**) Representative confocal images of HEK293T cells stably expressing YFP-Aβ42 (top row), α-synuclein containing the A53T mutation fused to YFP (α-syn(A53T)–YFP, middle row), or tauK18(LM)-YFP (bottom row) (see Materials and Methods for construct details). The cells were treated with APP-derived peptides from the brains of TgAPP23 mice (0.1 × PTA sample, left column), or Tgα-Syn*A53T mice (0.1 × PTA sample, middle column), or homozygous Tg0N4Rtau*P301S mice (0.1 × PTA sample, right column). Scale bar, 20 μm. (**B**) Quantification of the responses of the YFP-Aβ42, α-syn(A53T)-YFP, and tauK18(LM)-YFP cell lines 2 days after exposure to increasing concentrations of transgenic mouse brain–derived Aβ (0.01× to 0.1× PTA sample; orange to dark red), α-synuclein carrying the A53T mutation (0.01× to 0.1× PTA sample; light blue to dark blue), and tau carrying the P301S mutation (0.01 × to 0.1× PTA sample; light gray to dark gray). Data shown are means ± SEM as determined from four images per well across four wells and are representative of four independent experiments.

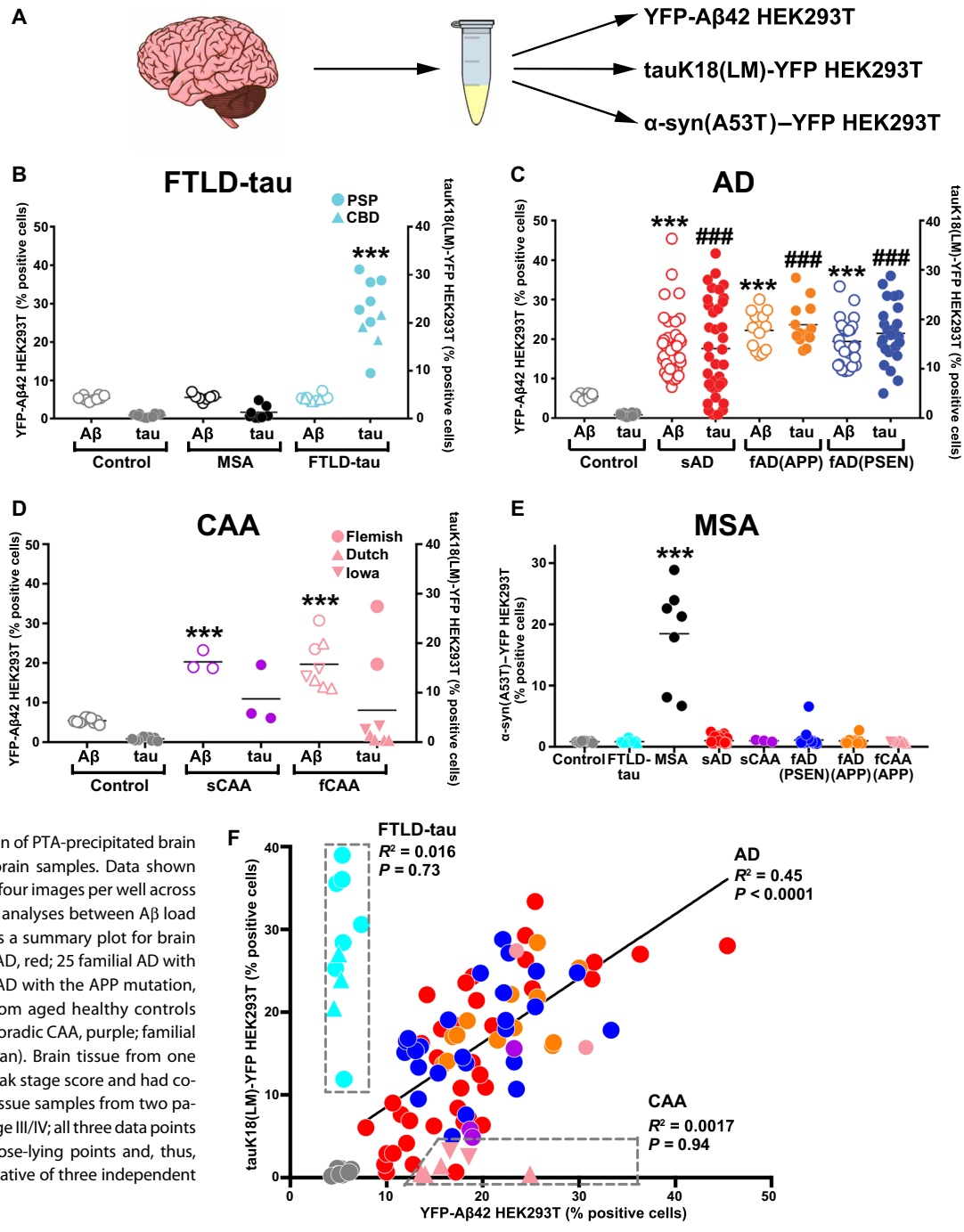


**Fig. 3. Quantitation of postmortem human brain Aβ and tau in parallel cellular assays.** (**A**) The prion-like activities of Aβ and tau in postmortem human brain samples from patients with FTLD-tau, AD, CAA, and MSA (multiple system atrophy) were added to three different HEK293T cell lines expressing YFP-Aβ42, tauK18(LM)-YFP, or α-syn(A53T)-YFP. (**B** to **D**) The prion-like activities of Aβ and tau in human brain tissue samples were quantified using the YFP-Aβ42 and tauK18(LM)-YFP cell lines. The cell lines were exposed to a 0.03× dilution of PTA-precipitated brain homogenates derived from 86 patients with sporadic or familial AD or CAA, 10 aged healthy controls, and 10 patients with FTLD-tau (7 with PSP and 3 with CBD). Data shown are means ± SEM as determined from four images per well across four wells per sample. Statistical significance is indicated as $^{***}P < 0.0001$ for Aβ puncta–inducing prion-like activity compared to control or $^{\#\#\#}P < 0.0001$ for tau puncta–inducing prion-like activity compared to control. (**E**) α-Synuclein abundance in brain homogenates was quantified as a percentage of α-syn(A53T)–YFP–expressing cells positive for α-synuclein puncta. The α-syn(A53T)–YFP cell line was exposed to a 0.03× dilution of PTA-precipitated brain homogenates from all postmortem brain samples. Data shown are means ± SEM as determined from four images per well across four wells per sample. (**F**) Correlation analyses between Aβ load (*x* axis) and tau load (*y* axis). Shown is a summary plot for brain tissue from 75 AD cases (37 sporadic AD, red; 25 familial AD with the PSEN mutation, blue; 13 familial AD with the APP mutation, orange) compared to brain tissue from aged healthy controls (gray) and from patients with CAA (sporadic CAA, purple; familial CAA, pink) or FTLD-tau (PSP/CBD, cyan). Brain tissue from one patient with sporadic AD lacked a Braak stage score and had comorbid Lewy body dementia; brain tissue samples from two patients with sporadic AD were Braak stage III/IV; all three data points fell well within the range of other close-lying points and, thus, were not removed. Data are representative of three independent experiments.

In familial CAA postmortem brain samples, Aβ puncta–inducing activity was uniformly elevated, whereas tau activity was either low or absent. Postmortem brain tissue from patients with AD carrying the Dutch (E22Q in Aβ or E693Q in APP) or Iowa (D22N) mutations showed substantial Aβ but insignificant tau puncta–inducing activity (Fig. 3D). Our findings are consistent with the absence of NFTs in the brains of these individuals (*17*, *18*). Elevated prion-like Aβ and tau activities were detected in postmortem brain tissue from two patients with CAA carrying the Flemish (A21G) mutation (Fig. 3D). This finding confirms earlier reports of widespread NFTs and hyperphosphorylated tau in dystrophic neurites in such patient cohorts (*53*, *54*). The two patients carrying the Flemish mutation (Fig. 3D) were slightly older at death (63 and 60 years old) than the patients carrying the Iowa and Dutch mutations (55.7 ± 2.9).

In a plot of prion-like Aβ versus tau in postmortem brain tissue from patients with different neurodegenerative diseases, the FTLD-tau cases were observed to lie near the *y* axis in a distinct region comprising very low Aβ (Fig. 3F); for these cases, there was no correlation between the prion-like Aβ and tau titers. Brain tissue from patients with familial CAA carrying the Dutch and Iowa mutations segregated along the *x* axis (Fig. 3F). The remaining brain samples were broadly distributed along the diagonal with a

modest but significant ($P < 0.0001$) linear correlation between prion-like Aβ and tau.

We next asked whether prion-like Aβ and tau activity in postmortem brain tissue at the time of death correlated with variables associated with the genetic background of the donor or the method of sample collection. No notable correlation was observed with respect to variables such as the type of brain bank and preservation method (table S1). However, correlations were observed between the longevity of the donor, the gender, and the genetic background of patients with AD despite the fact that all postmortem brain tissue had essentially the same confirmed neuropathology [Consortium to Establish a Registry for Alzheimer's Disease (CERAD) neuritic plaque, C3; Braak stages V and VI; table S1]. The values of f(Aβ) decreased modestly ($R^2 = 0.17$) with respect to longevity (Fig. 4, A and B), and f(tau) exhibited a similar linear decrease ($R^2 = 0.19$) with age (Fig. 4C). About half of the brain samples from patients who were 80 or older exhibited a low number of f(tau) puncta despite having reached Braak stage V or VI and CERAD score 3 (Fig. 4D). A preponderance of these elderly cases were female (fig. S5, A and B), although we cannot rule out collection bias as most of the elderly patient donors were female. Overall, these linear trends were observed in brain tissue samples from a broad range of patients with sporadic AD and patients with familial AD.

Given that the ε4 allele of the gene encoding apolipoprotein E (apoE) is the major risk factor for AD (*55*, *56*), we compared the effect of the *APOE* ε4 allele on the values of f(Aβ) and f(tau) (fig. S4, C and D). Correlation analysis showed that brain tissue from patients who were *APOE* ε4 noncarriers had lower quantities of tau aggregates than did brain tissue from *APOE* ε4 carriers, and this effect was particularly pronounced in patients over the age of 80 (fig. S4D). A similar trend was observed for Aβ, although this fell short of 95% statistical confidence ($P = 0.057$) for the given sample size (fig. S4C). Last, a weak correlation between f(tau) and brain region was observed for samples taken from the frontal and temporal lobes (fig. S4F).

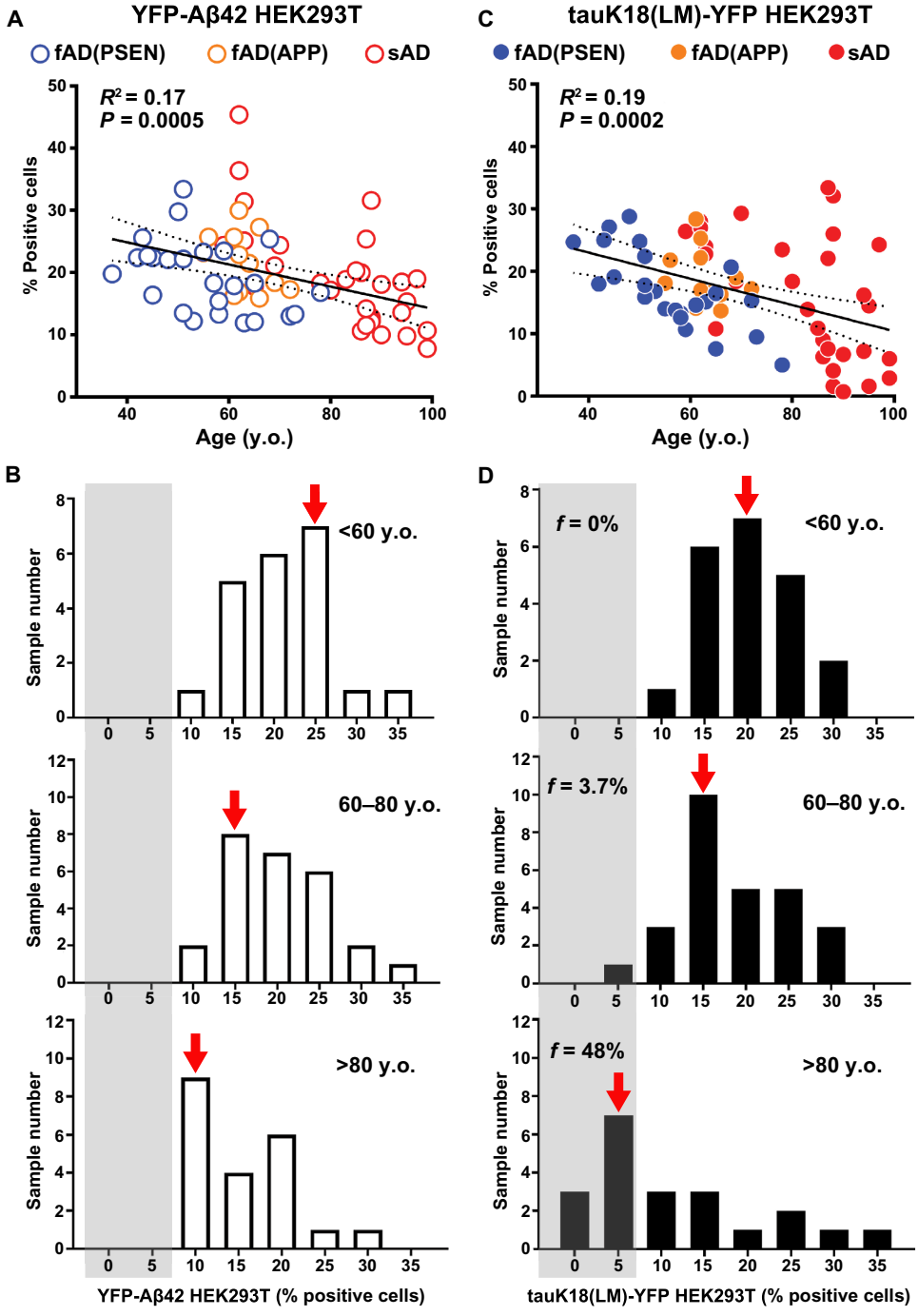


**Fig. 4. Inverse correlation between longevity and self-propagating Aβ and tau activities.** The Aβ and tau prion-like activity in brain tissue from sporadic and familial AD samples (Braak stages V and VI) was plotted as a function of patient age at death (**A**): familial AD with the *PSEN* mutation, blue; familial AD with the *APP* mutation, orange; sporadic AD, red. Statistical values for correlation, linear regression, and 95% confidence intervals are shown. (**B**) Histogram of Aβ load for the same dataset binned into three age groups: <60 years old (y.o., top); 60 to 80 years old (middle); and >80 years old (bottom). (**C**) Tau load in brain tissue from patients with sporadic AD and patients with familial AD plotted as a function of patient age at death: familial AD with the *PSEN* mutation, blue; familial AD with the *APP* mutation, orange; sporadic AD, red. Statistical values for correlation, linear regression, and 95% confidence intervals are shown. (**D**) Histogram of tau abundance for the same dataset binned into three age groups: <60 years old (top); 60 to 80 years old (middle); and >80 years old (bottom). Fraction of total sample number in each age bin with 0 to 5% tau-positive cells. The SDs of individual data points are similar to those in Fig. 1 and are much smaller than the deviation from the regression line, indicating that measurement error did not contribute significantly to the deviations from the trend line. Data are representative of three independent experiments.

### Correlations between longevity and APP, Aβ, tau, and phosphorylated tau

It is possible that the intersubject variations in the quantities of f(Aβ) and f(tau) simply reflect differences in *APP* and *MAPT* expression or the concentrations of misfolded forms of the proteins encoded by these genes. Alternatively, individuals with higher f(Aβ) and f(tau) might have biochemically or physically distinct forms exhibiting greater intrinsic stability or potency. To differentiate among these possibilities, we measured the total abundance of various forms of soluble and insoluble Aβ and tau in postmortem brain samples using ELISA. The abundance of APP, Aβ40, and Aβ42 showed a slight ($R^2$ = 0.12 to 0.23) but significant trend ($P$ < 0.005 in all cases) toward lower values with respect to age (Fig. 5, A to C).

Markedly different trends were observed when the abundance of various forms of the tau protein was quantified in postmortem brain samples. There was no significant relationship between age at death and concentrations of total soluble tau (Fig. 5D), as measured using an antibody that was specific for all splice forms of tau protein. Furthermore, the amount of total insoluble tau (Fig. 5E) increased with age in contrast to the decrease in prion-like tau activity shown in Fig. 4C. We therefore examined the abundance of insoluble phosphorylated tau (p-tau) in the postmortem brain samples because the amount of p-tau is known to be associated with clinical severity (*57*, *58*). Antibodies for three different p-tau epitopes (S396, S199, and T231) provided similar results: Each antibody showed that, unlike total insoluble tau, the extent of insoluble p-tau decreased linearly with age at death (Fig. 5F and fig. S5, B and C).

We next normalized prion-like tau abundance, relative to the total insoluble tau concentration, to provide a measure of the specific activity of the insoluble tau within a given brain sample. The data are described by an exponential decay ($R^2$ = 0.79) over five half-lives of observations. This correlation is in part a result of the data spanning a wide range of ages at death from 37 to 99 years, resulting in a large range of the dependent variables relative to sampling and other errors. If a smaller age range were considered, the overall range of specific activities would be smaller, while experimental and other errors would remain about the same, leading to a lower correlation coefficient. Thus, the exponential nature of the process is most clearly revealed by including as wide a range of ages as available.

The extent of tau phosphorylation as a function of age was similarly evaluated by calculating the amount of a given p-tau epitope in the insoluble tau fraction relative to total insoluble tau. Again, a single

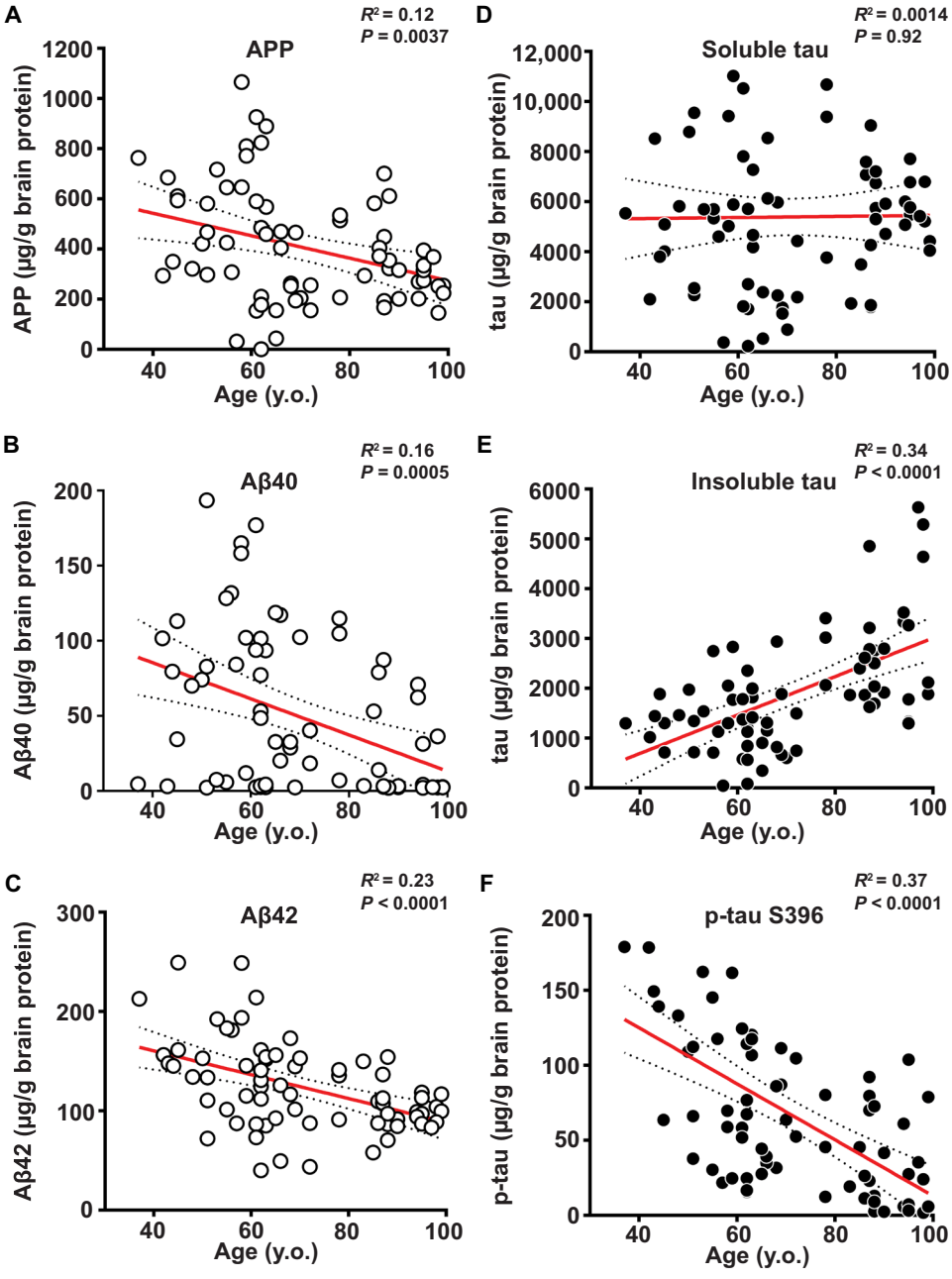


**Fig. 5. Measurement of APP expression and the amounts of soluble and insoluble Aβ and tau species as a function of the age at death of patients with AD.** ELISA was used to measure different proteins in brain samples (Braak stages V and VI) from patients with familial or sporadic AD. The following proteins were measured: (**A**) APP in the clarified brain homogenate (PBS soluble), (**B** and **C**) Aβ40 and Aβ42 (formic acid soluble), respectively, (**D**) total tau in the clarified brain homogenate (PBS soluble), (**E**) total tau (formic acid soluble), and (**F**) p-tau (phosphorylated epitope $Ser^{396}$, formic acid soluble). All data are plotted as a function of patient age at death. Statistical values for correlation, linear regression, and 95% confidence interval are shown. The measurements were made in duplicate and are much smaller than the deviation from the regression line, indicating that measurement error did not contribute significantly to the deviations from the trend line. Data are representative of one to two independent experiments.

exponential decay was observed over five half-lives, with $R^2$ values ranging from 0.75 to 0.78 ($P < 0.0001$), depending on the epitope used to quantify insoluble p-tau (Fig. 6, B to D). The half-life of prion-like tau obtained from the normalized cellular assay data (Fig. 6, A and E) was 12 years, whereas the corresponding half-lives for p-tau ranged from 7 to 10 years. The 95% confidence intervals for each of the half-lives overlapped (Fig. 6E), so it was not possible to distinguish whether the differences in half-lives were meaningful. At present, we can conclude that both prion-like tau activity and the extent of tau phosphorylation decreased about twofold for each decade of longevity. Thus, for example, on average, an individual who died at age 40 would have about $2^5$- or 32-fold higher prion-like tau than would an individual who lived five decades longer and died at age 90 (when normalized for total insoluble tau). Our data indicate that the biophysical and biochemical changes that accompany tau phosphorylation correlate with disease progression, and that prion-like activity rather than bulk accumulation of insoluble tau relates directly to longevity.

## DISCUSSION

A wealth of evidence argues that both Aβ and tau adopt pathological conformations leading to prion-like spreading throughout the brain during AD pathogenesis. The findings reported here establish the presence of both prion-like Aβ and prion-like tau proteins in the brains of patients who died of either sporadic or inherited AD. Moreover, studies by us and others in cellular and transgenic mouse models have previously demonstrated prion-like tau in the brains of patients who died of FTLD-tau (*36*, *38*, *59*–*61*). Our results extend those of earlier studies by demonstrating that postmortem brain tissue from patients with FTLD-tau was devoid of both prion-like Aβ and α-synuclein proteins (Fig. 3).

The linear trends in prion-like Aβ and tau with longevity were observed over a range of sporadic and familial forms of AD. Thus, what had appeared to be a set of disparate disorders can now be seen as a continuous spectrum, with the defining feature being the spreading of prion-like Aβ and tau through the CNS. Our findings from earlier molecular genetic studies and those described here begin to create a more complete view of the chemical processes that feature in the pathogenesis of AD, because they allow a clear definition between inactive inert tau and Aβ versus their active prion-like forms.

Both human and animal studies argue that pathologically misfolded Aβ initiates formation of prion-like tau (*18*, *21*, *62*, *63*) in AD. Presumably, the formation of prion-like Aβ begins in one or more brain regions and then spreads to others. The movement of $PrP^{Sc}$

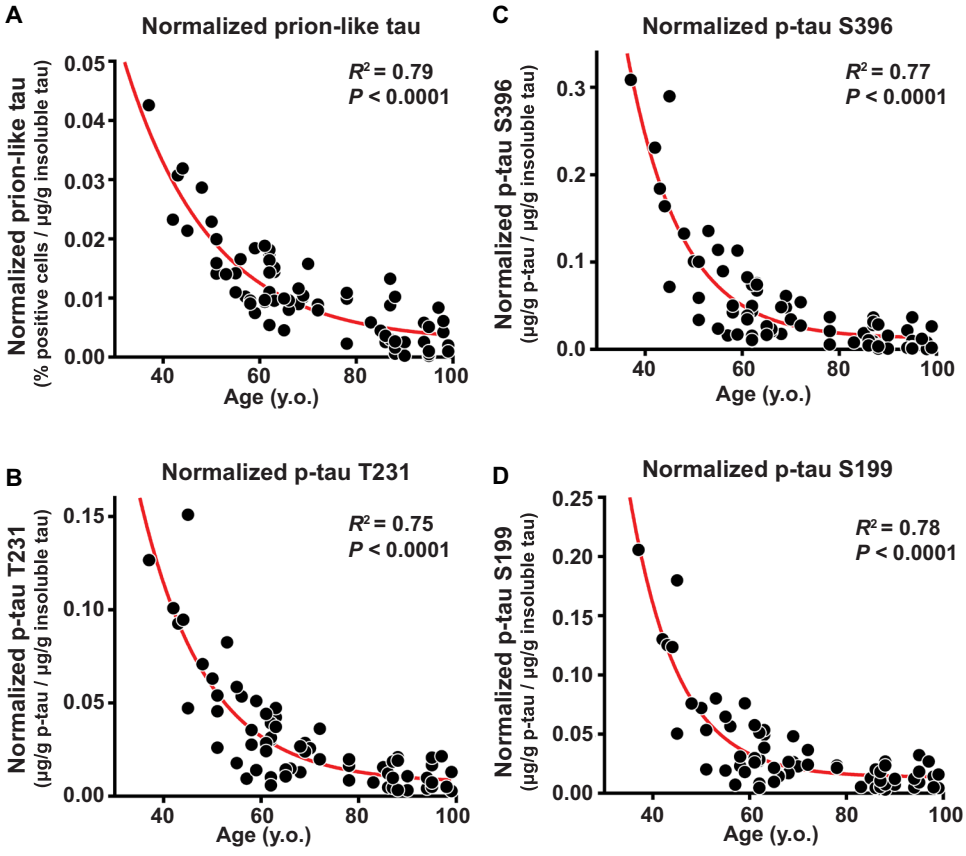


E

| Normalized to insoluble tau | *k* | *k* (95% CI) | $T_{1/2}$ | $T_{1/2}$ (95% CI) |
|---|---|---|---|---|
| prion-like tau | 0.06 | 0.04–0.07 | 12.4 | 9.3–17.8 |
| p-tau T231 | 0.07 | 0.05–0.09 | 9.5 | 7.4–12.6 |
| p-tau S396 | 0.09 | 0.07–0.11 | 7.7 | 6.1–9.8 |
| p-tau S199 | 0.1 | 0.08–0.12 | 6.9 | 5.6–8.7 |

**Fig. 6. The abundance of self-propagating and p-tau decreased exponentially over six decades in patients with AD.** The specific activity of prion-like tau in AD brain homogenates decreased in parallel with a reduction in hyperphosphorylated tau. (**A**) Prion-like tau abundance measured in AD brain tissue samples (Braak stages V and VI) was normalized to the adjusted value of insoluble tau as measured by ELISA (see Fig. 5E). Shown are normalized data plotted as a function of AD patient age at death and fitted using an exponential decay model equation (one-phase decay). (**B**) p-tau (phosphorylated on $Thr^{231}$; p-tauT231) was measured in AD brain samples normalized to the adjusted value of insoluble tau as measured by ELISA (see Fig. 5E). Normalized data were plotted as a function of AD patient age at death and fitted using an exponential decay model equation (one-phase decay). To normalize the data, the prion-like tau values from Fig. 4 or the p-tau concentration from Fig. 5 was divided by the concentration of total insoluble tau obtained from the regression line for total tau versus age at death for patients with AD shown in Fig. 5E. (**C**) p-tau (phosphorylated on $Ser^{396}$; p-tauS396) was measured in AD brain samples normalized to the adjusted value of insoluble tau as measured by ELISA. (**D**) p-tau (phosphorylated on $Ser^{199}$; p-tauS199) was measured in AD samples normalized to the adjusted value of insoluble tau as measured by ELISA. (**E**) Statistical values for correlation, decay constant (*k*), half-life (*T*), and their respective 95% confidence intervals (CIs) are shown.

prions and prion-like proteins such as α-synuclein, tau, and, possibly, Aβ42 from one CNS region to another argues for trans-synaptic spread (*64*–*69*). The apparent spread of prion-like proteins in the CNS is reflected by their regional distribution and has been well documented in neuropathological studies (*70*, *71*). The identification of distinct prion-like Aβ conformers in AD brain samples with different etiologies has been particularly informative (*72*–*75*). It remains to be determined which of these conformers are related to distinct disease phenotypes or which are associated with selective prion-like tau formation. Using the cellular assays reported here, we can now correlate the presence of a given conformer with prion-like tau or prion-like Aβ activities across a variety of phenotypic manifestations of AD.

Recent studies report that the minimal size of a biologically active tau aggregate may range from a monomer (*76*, *77*) to linear aggregates of ~100 nm in length (*78*). Pentameric or smaller tau aggregates were unable to support prion-like tau activity (*79*). Additionally, tau phosphorylation may also contribute to the conformation of prion-like tau as shown in previous studies where immunodepletion of p-tau in brain extracts used as inocula abolished prion-like tau activity in recipient cells (*80*, *81*) or in animal models (*79*). These findings are consistent with our data, demonstrating a relationship between prion-like tau activity and the extent of tau phosphorylation in brain samples from patients with AD obtained at different ages of death (Figs. 5 and 6).

Development of a new cellular assay for prion-like Aβ peptides has permitted us to compare prion-like Aβ generated using synthetic Aβ fibrils versus transgene-encoded Aβ preparations. Our cellular assay is useful for measuring Aβ prion-like activities generated by allele-specific Aβ subtypes. In addition, it has enabled parallel quantification of prion-like Aβ and prion-like tau activities, providing a direct quantitative comparison of these actively propagating species, rather than comparisons of inert protein deposits. Our data also show that the patients with AD with greatest longevity had lower concentrations of both prion-like Aβ and prion-like tau at the time of death compared to patients who died at younger ages from AD-related disease. Previous studies showed that the abundance of NFTs correlated well with the extent of brain atrophy and cognitive decline in AD (*29*, *82*). These studies focused only on total insoluble tau. By examining the age of death as a variable, we found that low prion-like tau activity correlated with greater longevity.

Both the extent of prion-like Aβ activity and the abundance of APP, Aβ40, and Aβ42 decreased with longevity in a roughly synchronous manner. This finding is consistent with the hypothesis that prion-like Aβ features early during the formation of pathological tau tangles. Moreover, measurable prion-like Aβ activity was found in the oldest patients, suggesting that it continues to participate throughout AD pathogenesis. However, the $R^2$ values that we found ranged from 0.12 to 0.2, indicating that many factors (from the methods of sample collection to genetic components) appeared to have a sizable influence on the observed correlation. Clearly, genetic factors such as the *APOE* ε4 allele and *TREM2* variants, which have been implicated in Aβ metabolism and clearance, can strongly increase the risk of AD (*56*, *83*). Although we found interesting trends with respect to the *APOE* ε4 genotype and gender, we will need to perform larger studies that carefully sample all of the different *APOE* genotypes.

The strong associations among longevity, prion-like tau activity, and tau phosphorylation are particularly intriguing. Such findings are consistent with the greater contribution of tau versus Aβ protein misfolding to the AD phenotype as measured by neurological dysfunction and neuropathological lesions. One particularly notable result is the accumulation of insoluble tau that increases with a greater age at death in contrast to insoluble p-tau, which decreases with increasing longevity (Figs. 4 and 5). Although these relationships were clear from examining the extent of prion-like tau formation and phosphorylation per gram of total brain protein, these findings became more notable when the data were normalized according to the abundance of insoluble tau (Fig. 6). Our findings argue that all insoluble tau is not equally neurotoxic and that biochemical events such as phosphorylation influence the formation of prion-like tau or modulate tau toxicity. It remains to be determined whether the low abundance of prion-like tau in long-lived patients with AD is a result of a slowly replicating tau conformer or is due to host factors that more readily clear prion-like conformers or shift prion-like tau toward a more inert amyloid state (e.g., total insoluble tau). Thus, future work aimed at the development of diagnostic reagents and effective therapeutics for AD will need to focus on prion-like tau activity and its associated posttranslational modifications rather than total insoluble tau.

Measuring both prion-like Aβ and prion-like tau abundance in postmortem brain samples is likely to have many applications. Antemortem detection of Aβ and tau activities in the CSF or blood of patients with AD, as shown for PrP prions (*84*–*86*), may provide more informative diagnostic tools to stage disease and measure efficacy of putative therapeutics. Also, our findings may help to illuminate both the successes and failures of pharmaceutical approaches that target Aβ and the Aβ-tau axis. The availability of paired cellular assays for measuring prion-like Aβ and prion-like tau should contribute to future drug discovery programs for AD.

## MATERIALS AND METHODS

### Study design

The aim of our study was to develop a rapid, quantitative cell-based assay to measure biologically active Aβ derived from postmortem human brain tissue. We first engineered HEK293T cell lines that were sensitive to Aβ40 and Aβ42 and validated the assay using synthetic Aβ fibrils that had previously been shown to be transmissible when injected into transgenic mouse brains (*33*, *34*). We tested our cell lines with these Aβ fibril preparations in three independent experiments. The sample size and time points (including end points) were chosen for cell and animal experiments based on our previous work (*34*, *37*, *38*, *75*). We used the minimum number of animals required to obtain a significant difference based on the expected variability, and all mice were randomly assigned and gender balanced. Deidentified human postmortem brain tissue was collected from several brain bank repositories located in the United States, Europe, and Australia (table S1). We replaced the identity of the samples with an internal code, and the investigator performing the experiments was blinded to the sample identity during testing and analysis. Experimental replicates for each experiment are listed in the figure legends.

### Cell line development

Constructs encoding human WT and mutant Aβ42 or Aβ40 fused with YFP at the N or C terminus were introduced into the pIRESpuro3 vector (Clontech), were transfected to HEK293T cells (American Type Culture Collection), and monoclonal cell lines were generated and

maintained as described (*37*). Cell lines expressing full-length human α-synuclein with the A53T mutation or human tau containing the repeat domain of 4R tau with the mutations P301L and V337 M fused with YFP were generated as described (*37*, *38*).

### Development of the cellular assay

The cellular bioassay for Aβ was developed as previously described (*37*, *38*). Briefly, cells were plated in a 384-well plate at a density of 3000 cells per well (70 μl per well) with Hoechst 33342 (0.1 μg/ml) (Thermo Fisher). A mixture of Lipofectamine 2000 (1.5% final volume, Thermo Fisher), OptiMEM (78.5% final volume, Thermo Fisher), and sample (20% final volume) was incubated at room temperature for 2 hours and plated in four replicate wells (10 μl per well). Plates were then incubated and imaged every 24 hours on the IN Cell Analyzer 6000 (GE Healthcare) for 3 to 4 days. Images of both the DAPI (4′,6-diamidino-2-phenylindole) and FITC (fluorescein isothiocyanate) channels were collected from four different regions in each well. The images were analyzed using the IN Cell Developer software with an algorithm developed to identify intracellular aggregates only in live cells.

### Preparation of synthetic Aβ fibrils

Preparation of synthetic Aβ fibrils was performed as described (*34*). Briefly, the WT Aβ40 and WT Aβ42 peptides were purchased from Bachem. Lyophilized peptides were dissolved to hexafluoroisopropanol (5 mg/ml) and separated in 200-μg aliquots. Hexafluoroisopropanol was evaporated in a SpeedVac and stored at −20°C. For conversion, the dried peptide film was solubilized in 20 μl of dimethyl sulfoxide and diluted with 980 μl of aqueous buffer solution containing 10 mM sodium phosphate. Samples were incubated at 37°C for 72 hours in 1.5-ml centrifugation tubes under constant agitation at 900 rpm. The resulting samples were spun down for 1 hour at 100,000*g*, and the pellet was resuspended in 100 μl of PBS at 2 mg/ml. Samples were further analyzed or diluted, snap frozen in liquid nitrogen, and stored at −80°C.

### PTA precipitation of Aβ peptides and tau proteins in postmortem brain samples

PTA precipitation of human postmortem brain samples was performed as described (*48*, *87*). Briefly, 10% brain homogenate was incubated in 2% sarkosyl and 0.5% benzonase (Sigma) at 37°C with constant agitation (1200 rpm) in an orbital shaker for 2 hours. Sodium PTA was dissolved in double-distilled $H_2O$ ($ddH_2O$), and the pH was adjusted to 7.0. PTA was added to the solution to a final concentration of 2%, which was then incubated overnight under the same conditions. The sample was centrifuged at 16,100*g* for 30 min at room temperature, and the supernatant was removed. The resulting pellet was resuspended in 2% sarkosyl in PBS and 2% PTA in $ddH_2O$ (pH 7.0). The sample was again incubated for at least 1 hour before a second centrifugation. The supernatant was again removed, and the pellet was resuspended in PBS using 10% of the initial starting volume and stored at −80°C.

To establish cellular assays for measuring prion-like Aβ and tau loads, we prepared a dilution series (e.g., 0.01, 0.03, and 0.1×) of all PTA-precipitated brain samples to perform the initial experiments. Once we established the dilution factor that best suited the majority of all samples, we performed subsequent experiments with only one or two dilution factors to conserve sample stocks. Using this approach, we ensured that our aggregation-inducing activity measurements were well within the dynamic range of the bioassay.

### Formic acid extraction of insoluble proteins in postmortem brain tissue for ELISA

Fifty microliters of formic acid was added to 25 μl of 10% brain homogenate and placed in an ultracentrifuge tube. The samples were vortexed, sonicated for 20 min at 37°C in a water-bath sonicator, and then centrifuged at 100,000*g* for 1 hour. We removed 50 μl of the supernatant and neutralized it with 950 μl of neutralization buffer in a low-binding tube. The neutralization buffer consisted of 1 M tris base and 500 mM dibasic sodium phosphate with no pH adjustment. (If a very small pellet or layer of lipids formed at the top of the supernatant, then we aspirated the sample from the middle of the supernatant to maximize the protein in the extract.) Samples were aliquoted into low-binding tubes and flash frozen in liquid nitrogen. The following ELISA kits from Thermo Fisher Scientific were used according to the manufacturer's protocol: APP (KHB0051), Aβ40 (KHB3481), Aβ42 (KHB3441), total tau (KHB0041), p-tau S396 (KHB7031), p-tau S199 (KHB7041), and p-tau T231 (KHB8051). The Aβ43 ELISA kit was from IBL-America (27710). Each sample was analyzed in duplicate. We adjusted the raw ELISA values to total brain protein (grams) in the clarified 10% brain homogenate as determined by bicinchoninic acid assay (Pierce/Thermo Fisher Scientific).

### Transgenic mice

TgAPP23 mice, which express human APP (751–amino acid isoform) containing the Swedish mutation under the control of the *Thy-1.2* promoter, were maintained on a C57BL/6 background. TgCRND8 mice, which express human APP (695–amino acid isoform) with the Swedish and Indiana mutations under the control of the hamster *Prnp* promoter, were maintained on a mixed B6/C3 background. Tg*Gfap*-luc mice, which express firefly luciferase under the control of the murine *Gfap* promoter, were a gift from Caliper Life Sciences and were maintained on an FVB/N background. To create bigenic mice, TgAPP23 and TgCRND8 mice were crossed with Tg*Gfap*-luc animals and were screened for the presence of both transgenes. Aged homozygous Tg0N4Rtau*P301S ("Tg2541$^{+/+}$") and Tgα-Syn*A53T ("TgM83$^{+/+}$") mice were used to provide control brain samples (*50*, *51*). Animals were maintained in an Association for Assessment and Accreditation of Laboratory Animal Care International–accredited facility in accordance with the *Guide for the Care and Use of Laboratory Animals*. All procedures were approved by the Institutional Animal Care and Use Committee of the University of California, San Francisco.

### Bioluminescence imaging

Bioluminescence imaging of the brains of bigenic TgAPP23:*Gfap*-luc mice and TgCRND8:*Gfap*-luc mice was performed as previously described (*32*). Isoflurane-anesthetized, head-shaved mice were imaged (60-s exposure) after receiving an intraperitoneal injection of 50 μl of D-luciferin potassium salt solution (30 mg/ml; Gold Biotechnology) that was prepared in PBS (pH 7.4) (a dose of ~60 mg/kg). Brain bioluminescence values were calculated from images displaying surface radiance using circular regions of interest and then were converted to total photon flux (photons per second) using Living Image software version 4.4 (PerkinElmer).

### Statistical analysis

Statistical analyses were performed with GraphPad Prism version 7. Data are shown as means ± SEM. Comparisons between multiple groups were performed using one-way analysis of variance (ANOVA) with post hoc Dunnett's test. We used linear regression analysis for

correlation plots. For two-group (frequency distribution) comparisons, we used a nonparametric Mann-Whitney *U* test. A value of $P < 0.05$ was considered significant. The exponential decay equation model (one-phase decay) used the least-squares (ordinary) fitting method with no constraints applied.

## SUPPLEMENTARY MATERIALS

stm.sciencemag.org/cgi/content/full/11/490/eaat8462/DC1

Fig. S1. Development of YFP-Aβ fusion HEK293T cell lines: Synthetic Aβ fibril inocula- and puncta-inducing kinetics.

Fig. S2. Development of YFP-Aβ fusion HEK293T cell lines: Individual clones.

Fig. S3. Amyloid plaque pathology, astrogliosis, and prion-like Aβ abundance during disease progression in TgAPP23 and TgCRND8 mice.

Fig. S4. *APOE* ε4 status, gender, and brain region influence the extent of prion-like Aβ and tau abundance in AD postmortem brain tissue.

Fig. S5. Correlation of different Aβ and tau species with age at death of patients with AD.

Table S1. Source of postmortem human brain tissue samples.

Data file S1. Source data.

## REFERENCES AND NOTES


1. A. Alzheimer, Über eigenartige Krankheitsfälle des späteren Alters. *Zentralbl. Gesamte Neurol. Psychiatr.* **4**, 356–385 (1911).
2. G. G. Glenner, C. W. Wong, Alzheimer's disease: Initial report of the purification and characterization of a novel cerebrovascular amyloid protein. *Biochem. Biophys. Res. Commun.* **120**, 885–890 (1984).
3. J. P. Brion, A. M. Couck, E. Passareiro, J. Flament-Durand, Neurofibrillary tangles of Alzheimer's disease: An immunohistochemical study. *J. Submicrosc. Cytol.* **17**, 89–96 (1985).
4. I. Grundke-Iqbal, K. Iqbal, Y. C. Tung, M. Quinlan, H. M. Wisniewski, L. I. Binder, Abnormal phosphorylation of the microtubule-associated protein tau (tau) in Alzheimer cytoskeletal pathology. *Proc. Natl. Acad. Sci. U.S.A.* **83**, 4913–4917 (1986).
5. K. S. Kosik, C. L. Joachim, D. J. Selkoe, Microtubule-associated protein tau (tau) is a major antigenic component of paired helical filaments in Alzheimer disease. *Proc. Natl. Acad. Sci. U.S.A.* **83**, 4044–4048 (1986).
6. N. J. Pollock, S. S. Mirra, L. I. Binder, L. A. Hansen, J. G. Wood, Filamentous aggregates in Pick's disease, progressive supranuclear palsy, and Alzheimer's disease share antigenic determinants with microtubule-associated protein tau. *Lancet* **2**, 1211 (1986).
7. J. I. Ayers, B. I. Giasson, D. R. Borchelt, Prion-like spreading in tauopathies. *Biol. Psychiatry* **83**, 337–346 (2018).
8. C. Condello, J. Stöehr, Aβ propagation and strains: Implications for the phenotypic diversity in Alzheimer's disease. *Neurobiol. Dis.* **109**, 191–200 (2018).
9. S. B. Prusiner, A unifying role for prions in neurodegenerative diseases. *Science* **336**, 1511–1513 (2012).
10. S. B. Prusiner, in *Prion Biology*, S. B. Prusiner, Ed. (Cold Spring Harbor Laboratory Press, 2017), pp. 1–15.
11. K. Hsiao, H. F. Baker, T. J. Crow, M. Poulter, F. Owen, J. D. Terwilliger, D. Westaway, J. Ott, S. B. Prusiner, Linkage of a prion protein missense variant to Gerstmann-Sträussler syndrome. *Nature* **338**, 342–345 (1989).
12. A. Goate, M. C. Chartier-Harlin, M. Mullan, J. Brown, F. Crawford, L. Fidani, L. Giuffra, A. Haynes, N. Irving, L. James, R. Mant, P. Newton, K. Rooke, P. Roques, C. Talbot, M. Pericak-Vance, A. Roses, R. Williamson, M. Rossor, M. Owen, J. Hardy, Segregation of a missense mutation in the amyloid precursor protein gene with familial Alzheimer's disease. *Nature* **349**, 704–706 (1991).
13. A. Goate, J. Hardy, Twenty years of Alzheimer's disease-causing mutations. *J. Neurochem.* **120** (Suppl. 1), 3–8 (2012).
14. J. TCW, A. M. Goate, in *Prion Diseases*, S. B. Prusiner, Ed. (Cold Spring Harbor Laboratory Press, 2017), pp. 203–213.
15. M. Hutton, C. L. Lendon, P. Rizzu, M. Baker, S. Froelich, H. Houlden, S. Pickering-Brown, S. Chakraverty, A. Isaacs, A. Grover, J. Hackett, J. Adamson, S. Lincoln, D. Dickson, P. Davies, R. C. Petersen, M. Stevens, E. de Graaff, E. Wauters, J. van Baren, M. Hillebrand, M. Joosse, J. M. Kwon, P. Nowotny, L. K. Che, J. Norton, J. C. Morris, L. A. Reed, J. Trojanowski, H. Basun, L. Lannfelt, M. Neystat, S. Fahn, F. Dark, T. Tannenberg, P. R. Dodd, N. Hayward, J. B. J. Kwok, P. R. Schofield, A. Andreadis, J. Snowden, D. Craufurd, D. Neary, F. Owen, B. A. Oostra, J. Hardy, A. Goate, J. van Swieten, D. Mann, T. Lynch, P. Heutink, Association of missense and 5′-splice-site mutations in tau with the inherited dementia FTDP-17. *Nature* **393**, 702–705 (1998).
16. M. G. Spillantini, T. D. Bird, B. Ghetti, Frontotemporal dementia and parkinsonism linked to chromosome 17: A new group of tauopathies. *Brain Pathol.* **8**, 387–402 (1998).
17. S. G. Van Duinen, E. M. Castaño, F. Prelli, G. T. Bots, W. Luyendijk, B. Frangione, Hereditary cerebral hemorrhage with amyloidosis in patients of Dutch origin is related to Alzheimer disease. *Proc. Natl. Acad. Sci. U.S.A.* **84**, 5991–5994 (1987).
18. M. L. Maat-Schieman, H. Yamaguchi, I. M. Hegeman-Kleinn, C. Welling-Graafland, R. Natté, R. A. C. Roos, S. G. van Duinen, Glial reactions and the clearance of amyloid β protein in the brains of patients with hereditary cerebral hemorrhage with amyloidosis-Dutch type. *Acta Neuropathol.* **107**, 389–398 (2004).
19. K. L. Viola, W. L. Klein, Amyloid β oligomers in Alzheimer's disease pathogenesis, treatment, and diagnosis. *Acta Neuropathol.* **129**, 183–206 (2015).
20. E. Karran, B. De Strooper, The amyloid cascade hypothesis: Are we poised for success or failure? *J. Neurochem.* **139** (Suppl. 2), 237–252 (2016).
21. J. Gotz, F. Chen, J. van Dorpe, R. M. Nitsch, Formation of neurofibrillary tangles in P301l tau transgenic mice induced by Abeta 42 fibrils. *Science* **293**, 1491–1495 (2001).
22. J. Lewis, D. W. Dickson, W. L. Lin, L. Chisholm, A. Corral, G. Jones, S. H. Yen, N. Sahara, L. Skipper, D. Yager, C. Eckman, J. Hardy, M. Hutton, E. McGowan, Enhanced neurofibrillary degeneration in transgenic mice expressing mutant tau and APP. *Science* **293**, 1487–1491 (2001).
23. R. E. Bennett, S. L. DeVos, S. Dujardin, B. Corjuc, R. Gor, J. Gonzalez, A. D. Roe, M. P. Frosch, R. Pitstick, G. A. Carlson, B. T. Hyman, Enhanced tau aggregation in the presence of amyloid β. *Am. J. Pathol.* **187**, 1601–1612 (2017).
24. Z. He, J. L. Guo, J. D. McBride, S. Narasimhan, H. Kim, L. Changolkar, B. Zhang, R. J. Gathagan, C. Yue, C. Dengler, A. Stieber, M. Nitla, D. A. Coulter, T. Abel, K. R. Brunden, J. Q. Trojanowski, V. M. Lee, Amyloid-β plaques enhance Alzheimer's brain tau-seeded pathologies by facilitating neuritic plaque tau aggregation. *Nat. Med.* **24**, 29–38 (2018).
25. S. E. Lesne, Toxic oligomer species of amyloid-β in Alzheimer's disease, a timing issue. *Swiss Med. Wkly.* **144**, w14021 (2014).
26. E. S. Musiek, D. M. Holtzman, Three dimensions of the amyloid hypothesis: Time, space and 'wingmen'. *Nat. Neurosci.* **18**, 800–806 (2015).
27. D. R. Thal, U. Rüb, M. Orantes, H. Braak, Phases of Aβ-deposition in the human brain and its relevance for the development of AD. *Neurology* **58**, 1791–1800 (2002).
28. M. E. Murray, V. J. Lowe, N. R. Graff-Radford, A. M. Liesinger, A. Cannon, S. A. Przybelski, B. Rawal, J. E. Parisi, R. C. Petersen, K. Kantarci, O. A. Ross, R. Duara, D. S. Knopman, C. R. Jack Jr., D. W. Dickson, Clinicopathologic and $^{11}$C-Pittsburgh compound B implications of Thal amyloid phase across the Alzheimer's disease spectrum. *Brain* **138**, 1370–1381 (2015).
29. C. R. Jack Jr., D. S. Knopman, W. J. Jagust, R. C. Petersen, M. W. Weiner, P. S. Aisen, L. M. Shaw, P. Vemuri, H. J. Wiste, S. D. Weigand, T. G. Lesnick, V. S. Pankratz, M. C. Donohue, J. Q. Trojanowski, Tracking pathophysiological processes in Alzheimer's disease: An updated hypothetical model of dynamic biomarkers. *Lancet Neurol.* **12**, 207–216 (2013).
30. M. Meyer-Luehmann, J. Coomaraswamy, T. Bolmont, S. Kaeser, C. Schaefer, E. Kilger, A. Neuenschwander, D. Abramowski, P. Frey, A. L. Jaton, J. M. Vigouret, P. Paganetti, D. M. Walsh, P. M. Mathews, J. Ghiso, M. Staufenbiel, L. C. Walker, M. Jucker, Exogenous induction of cerebral beta-amyloidogenesis is governed by agent and host. *Science* **313**, 1781–1784 (2006).
31. Y. S. Eisele, U. Obermuller, G. Heilbronner, F. Baumann, S. A. Kaeser, H. Wolburg, L. C. Walker, M. Staufenbiel, M. Heikenwalder, M. Jucker, Peripherally applied Aβ-containing inoculates induce cerebral beta-amyloidosis. *Science* **330**, 980–982 (2010).
32. J. C. Watts, K. Giles, S. K. Grillo, A. Lemus, S. J. DeArmond, S. B. Prusiner, Bioluminescence imaging of Aβ deposition in bigenic mouse models of Alzheimer's disease. *Proc. Natl. Acad. Sci. U.S.A.* **108**, 2528–2533 (2011).
33. J. Stöhr, J. C. Watts, Z. L. Mensinger, A. Oehler, S. K. Grillo, S. J. DeArmond, S. B. Prusiner, K. Giles, Purified and synthetic Alzheimer's amyloid beta (Aβ) prions. *Proc. Natl. Acad. Sci. U.S.A.* **109**, 11025–11030 (2012).
34. J. Stöhr, C. Condello, J. C. Watts, L. Bloch, A. Oehler, M. Nick, S. J. DeArmond, K. Giles, W. F. DeGrado, S. B. Prusiner, Distinct synthetic Aβ prion strains producing different amyloid deposits in bigenic mice. *Proc. Natl. Acad. Sci. U.S.A.* **111**, 10329–10334 (2014).
35. N. Kfoury, B. B. Holmes, H. Jiang, D. M. Holtzman, M. I. Diamond, Trans-cellular propagation of tau aggregation by fibrillar species. *J. Biol. Chem.* **287**, 19440–19451 (2012).
36. D. W. Sanders, S. K. Kaufman, S. L. DeVos, A. M. Sharma, H. Mirbaha, A. Li, S. J. Barker, A. C. Foley, J. R. Thorpe, L. C. Serpell, T. M. Miller, L. T. Grinberg, W. W. Seeley, M. I. Diamond, Distinct tau prion strains propagate in cells and mice and define different tauopathies. *Neuron* **82**, 1271–1288 (2014).
37. A. L. Woerman, J. Stöhr, A. Aoyagi, R. Rampersaud, Z. Krejciova, J. C. Watts, T. Ohyama, S. Patel, K. Widjaja, A. Oehler, D. W. Sanders, M. I. Diamond, W. W. Seeley, L. T. Middleton, S. M. Gentleman, D. A. Mordes, T. C. Südhof, K. Giles, S. B. Prusiner, Propagation of prions causing synucleinopathies in cultured cells. *Proc. Natl. Acad. Sci. U.S.A.* **112**, E4949–E4958 (2015).
38. A. L. Woerman, A. Aoyagi, S. Patel, S. A. Kazmi, I. Lobach, L. T. Grinberg, A. C. McKee, W. W. Seeley, S. H. Olson, S. B. Prusiner, Tau prions from Alzheimer's disease and chronic traumatic encephalopathy patients propagate in cultured cells. *Proc. Natl. Acad. Sci. U.S.A.* **113**, E8187–E8196 (2016).

39. C. Wurth, N. K. Guimard, M. H. Hecht, Mutations that reduce aggregation of the Alzheimer's Aβ42 peptide: An unbiased search for the sequence determinants of Aβ amyloidogenesis. *J. Mol. Biol.* **319**, 1279–1290 (2002).
40. W. Kim, Y. Kim, J. Min, D. J. Kim, Y. T. Chang, M. H. Hecht, A high-throughput screen for compounds that inhibit aggregation of the Alzheimer's peptide. *ACS Chem. Biol.* **1**, 461–469 (2006).
41. T. Ochiishi, M. Doi, K. Yamasaki, K. Hirose, A. Kitamura, T. Urabe, N. Hattori, M. Kinjo, T. Ebihara, H. Shimura, Development of new fusion proteins for visualizing amyloid-β oligomers in vivo. *Sci. Rep.* **6**, 22712 (2016).
42. J. X. Lu, W. Qiang, W. M. Yau, C. D. Schwieters, S. C. Meredith, R. Tycko, Molecular structure of β-amyloid fibrils in Alzheimer's disease brain tissue. *Cell* **154**, 1257–1268 (2013).
43. M. Schmidt, A. Rohou, K. Lasker, J. K. Yadav, C. Schiene-Fischer, M. Fändrich, N. Grigorieff, Peptide dimer structure in an Aβ(1-42) fibril visualized with cryo-EM. *Proc. Natl. Acad. Sci. U.S.A.* **112**, 11858–11863 (2015).
44. L. Gremer, D. Schölzel, C. Schenk, E. Reinartz, J. Labahn, R. B. G. Ravelli, M. Tusche, C. Lopez-Iglesias, W. Hoyer, H. Heise, D. Willbold, G. F. Schröder, Fibril structure of amyloid-β(1-42) by cryo-electron microscopy. *Science* **358**, 116–119 (2017).
45. C. Nilsberth, A. Westlind-Danielsson, C. B. Eckman, M. M. Condron, K. Axelman, C. Forsell, C. Stenh, J. Luthman, D. B. Teplow, S. G. Younkin, J. Näslund, L. Lannfelt, The 'Arctic' APP mutation (E693G) causes Alzheimer's disease by enhanced Aβ protofibril formation. *Nat. Neurosci.* **4**, 887–893 (2001).
46. M. R. Elkins, T. Wang, M. Nick, H. Jo, T. Lemmin, S. B. Prusiner, W. F. DeGrado, J. Stöhr, M. Hong, Structural polymorphism of Alzheimer's β-amyloid fibrils as controlled by an E22 switch: A solid-state NMR study. *J. Am. Chem. Soc.* **138**, 9840–9852 (2016).
47. A. L. Cloe, J. P. Orgel, J. R. Sachleben, R. Tycko, S. C. Meredith, The Japanese mutant Aβ (ΔE22-Aβ(1-39)) forms fibrils instantaneously, with low-thioflavin T fluorescence: Seeding of wild-type Aβ(1-40) into atypical fibrils by ΔE22-Aβ(1-39). *Biochemistry* **50**, 2026–2039 (2011).
48. D. J. Levine, J. Stöhr, L. E. Falese, J. Ollesch, H. Wille, S. B. Prusiner, J. R. Long, Mechanism of scrapie prion precipitation with phosphotungstate anions. *ACS Chem. Biol.* **10**, 1269–1277 (2015).
49. C. Sturchler-Pierrat, D. Abramowski, M. Duke, K. H. Wiederhold, C. Mistl, S. Rothacher, B. Ledermann, K. Burki, P. Frey, P. A. Paganetti, C. Waridel, M. E. Calhoun, M. Jucker, A. Probst, M. Staufenbiel, B. Sommer, Two amyloid precursor protein transgenic mouse models with Alzheimer disease-like pathology. *Proc. Natl. Acad. Sci. U.S.A.* **94**, 13287–13292 (1997).
50. B. Allen, E. Ingram, M. Takao, M. J. Smith, R. Jakes, K. Virdee, H. Yoshida, M. Holzer, M. Craxton, P. C. Emson, C. Atzori, A. Migheli, R. A. Crowther, B. Ghetti, M. G. Spillantini, M. Goedert, Abundant tau filaments and nonapoptotic neurodegeneration in transgenic mice expressing human P301S tau protein. *J. Neurosci.* **22**, 9340–9351 (2002).
51. B. I. Giasson, J. E. Duda, S. M. Quinn, B. Zhang, J. Q. Trojanowski, V. M. Y. Lee, Neuronal α-synucleinopathy with severe movement disorder in mice expressing A53T human α-synuclein. *Neuron* **34**, 521–533 (2002).
52. M. A. Chishti, D. S. Yang, C. Janus, A. L. Phinney, P. Horne, J. Pearson, R. Strome, N. Zuker, J. Loukides, J. French, S. Turner, G. Lozza, M. Grilli, S. Kunicki, C. Morissette, J. Paquette, F. Gervais, C. Bergeron, P. E. Fraser, G. A. Carlson, P. S. George-Hyslop, D. Westaway, Early-onset amyloid deposition and cognitive deficits in transgenic mice expressing a double mutant form of amyloid precursor protein 695. *J. Biol. Chem.* **276**, 21562–21570 (2001).
53. P. Cras, F. van Harskamp, L. Hendriks, C. Ceuterick, C. M. van Duijn, S. Z. Stefanko, A. Hofman, J. M. Kros, C. van Broeckhoven, J. J. Martin, F. van Harskamp, Presenile Alzheimer dementia characterized by amyloid angiopathy and large amyloid core type senile plaques in the APP 692Ala-->Gly mutation. *Acta Neuropathol.* **96**, 253–260 (1998).
54. S. Kumar-Singh, P. Cras, R. Wang, J. M. Kros, J. van Swieten, U. Lübke, C. Ceuterick, S. Serneels, K. Vennekens, J. P. Timmermans, E. van Marck, J. J. Martin, C. M. van Duijn, C. van Broeckhoven, Dense-core senile plaques in the Flemish variant of Alzheimer's disease are vasocentric. *Am. J. Pathol.* **161**, 507–520 (2002).
55. P. B. Verghese, J. M. Castellano, D. M. Holtzman, Apolipoprotein E in Alzheimer's disease and other neurological disorders. *Lancet Neurol.* **10**, 241–252 (2011).
56. N. Zhao, C.-C. Liu, W. Qiao, G. Bu, Apolipoprotein E, receptors, and modulation of Alzheimer's disease. *Biol. Psychiatry* **83**, 347–357 (2018).
57. J. C. Augustinack, A. Schneider, E. M. Mandelkow, B. T. Hyman, Specific tau phosphorylation sites correlate with severity of neuronal cytopathology in Alzheimer's disease. *Acta Neuropathol.* **103**, 26–35 (2002).
58. H. Braak, I. Alafuzoff, T. Arzberger, H. Kretzschmar, K. Del Tredici, Staging of Alzheimer disease-associated neurofibrillary pathology using paraffin sections and immunocytochemistry. *Acta Neuropathol.* **112**, 389–404 (2006).
59. F. Clavaguera, T. Bolmont, R. A. Crowther, D. Abramowski, S. Frank, A. Probst, G. Fraser, A. K. Stalder, M. Beibel, M. Staufenbiel, M. Jucker, M. Goedert, M. Tolnay, Transmission and spreading of tauopathy in transgenic mouse brain. *Nat. Cell Biol.* **11**, 909–913 (2009).
60. B. Frost, R. L. Jacks, M. I. Diamond, Propagation of tau misfolding from the outside to the inside of a cell. *J. Biol. Chem.* **284**, 12845–12852 (2009).
61. A. L. Woerman, S. Patel, S. A. Kazmi, A. Oehler, Y. Freyman, L. Espiritu, R. Cotter, J. A. Castaneda, S. H. Olson, S. B. Prusiner, Kinetics of human mutant tau prion formation in the brains of 2 transgenic mouse lines. *JAMA Neurol.* **74**, 1464–1472 (2017).
62. T. Bolmont, F. Clavaguera, M. Meyer-Luehmann, M. C. Herzig, R. Radde, M. Staufenbiel, J. Lewis, M. Hutton, M. Tolnay, M. Jucker, Induction of tau pathology by intracerebral infusion of amyloid-beta -containing brain extract and by amyloid-beta deposition in APP x tau transgenic mice. *Am. J. Pathol.* **171**, 2012–2020 (2007).
63. B. Vasconcelos, I. C. Stancu, A. Buist, M. Bird, P. Wang, A. Vanoosthuyse, K. van Kolen, A. Verheyen, P. Kienlen-Campard, J. N. Octave, P. Baatsen, D. Moechars, I. Dewachter, Heterotypic seeding of tau fibrillization by pre-aggregated Abeta provides potent seeds for prion-like seeding and propagation of tau-pathology in vivo. *Acta Neuropathol.* **131**, 549–569 (2016).
64. J. H. Kordower, Y. Chu, R. A. Hauser, T. B. Freeman, C. W. Olanow, Lewy body-like pathology in long-term embryonic nigral transplants in Parkinson's disease. *Nat. Med.* **14**, 504–506 (2008).
65. J. Y. Li, E. Englund, J. L. Holton, D. Soulet, P. Hagell, A. J. Lees, T. Lashley, N. P. Quinn, S. Rehncrona, A. Björklund, H. Widner, T. Revesz, O. Lindvall, P. Brundin, Lewy bodies in grafted neurons in subjects with Parkinson's disease suggest host-to-graft disease propagation. *Nat. Med.* **14**, 501–503 (2008).
66. P. Desplats, H. J. Lee, E. J. Bae, C. Patrick, E. Rockenstein, L. Crews, B. Spencer, E. Masliah, S. J. Lee, Inclusion formation and neuronal cell death through neuron-to-neuron transmission of alpha-synuclein. *Proc. Natl. Acad. Sci. U.S.A.* **106**, 13010–13015 (2009).
67. M. Iba, J. D. McBride, J. L. Guo, B. Zhang, J. Q. Trojanowski, V. M. Y. Lee, Tau pathology spread in PS19 tau transgenic mice following locus coeruleus (LC) injections of synthetic tau fibrils is determined by the LC's afferent and efferent connections. *Acta Neuropathol.* **130**, 349–362 (2015).
68. L. Ye, T. Hamaguchi, S. K. Fritschi, Y. S. Eisele, U. Obermüller, M. Jucker, L. C. Walker, Progression of seed-induced Aβ deposition within the limbic connectome. *Brain Pathol.* **25**, 743–752 (2015).
69. J. W. Wu, S. A. Hussaini, I. M. Bastille, G. A. Rodriguez, A. Mrejeru, K. Rilett, D. W. Sanders, C. Cook, H. Fu, R. A. C. M. Boonen, M. Herman, E. Nahmani, S. Emrani, Y. H. Figueroa, M. I. Diamond, C. L. Clelland, S. Wray, K. E. Duff, Neuronal activity enhances tau propagation and tau pathology in vivo. *Nat. Neurosci.* **19**, 1085–1092 (2016).
70. H. Braak, E. Braak, D. Yilmazer, R. A. I. de Vos, E. N. H. Jansen, J. Bohl, Pattern of brain destruction in Parkinson's and Alzheimer's diseases. *J. Neural Transm.* **103**, 455–490 (1996).
71. H. Braak, K. Del Tredici, in *Prion Biology*, S. B. Prusiner, Ed. (Cold Spring Harbor Laboratory Press, 2017), pp. 377–399.
72. J. C. Watts, C. Condello, J. Stohr, A. Oehler, J. Lee, S. J. DeArmond, L. Lannfelt, M. Ingelsson, K. Giles, S. B. Prusiner, Serial propagation of distinct strains of Aβ prions from Alzheimer's disease patients. *Proc. Natl. Acad. Sci. U.S.A.* **111**, 10323–10328 (2014).
73. W. Qiang, W. M. Yau, J. X. Lu, J. Collinge, R. Tycko, Structural variation in amyloid-β fibrils from Alzheimer's disease clinical subtypes. *Nature* **541**, 217–221 (2017).
74. J. Rasmussen, J. Mahler, N. Beschorner, S. A. Kaeser, L. M. Häsler, F. Baumann, S. Nyström, E. Portelius, K. Blennow, T. Lashley, N. C. Fox, D. Sepulveda-Falla, M. Glatzel, A. L. Oblak, B. Ghetti, K. P. R. Nilsson, P. Hammarström, M. Staufenbiel, L. C. Walker, M. Jucker, Amyloid polymorphisms constitute distinct clouds of conformational variants in different etiological subtypes of Alzheimer's disease. *Proc. Natl. Acad. Sci. U.S.A.* **114**, 13018–13023 (2017).
75. C. Condello, T. Lemmin, J. Stöhr, M. Nick, Y. Wu, A. M. Maxwell, J. C. Watts, C. D. Caro, A. Oehler, C. D. Keene, T. D. Bird, S. G. van Duinen, L. Lannfelt, M. Ingelsson, C. Graff, K. Giles, W. F. DeGrado, S. B. Prusiner, Structural heterogeneity and intersubject variability of Aβ in familial and sporadic Alzheimer's disease. *Proc. Natl. Acad. Sci. U.S.A.* **115**, E782–E791 (2018).
76. H. Mirbaha, D. Chen, O. A. Morazova, K. M. Ruff, A. M. Sharma, X. Liu, M. Goodarzi, R. V. Pappu, D. W. Colby, H. Mirzaei, L. A. Joachimiak, M. I. Diamond, Inert and seed-competent tau monomers suggest structural origins of aggregation. *eLife* **7**, e36584 (2018).
77. A. M. Sharma, T. L. Thomas, D. R. Woodard, O. M. Kashmer, M. I. Diamond, Tau monomer encodes strains. *eLife* **7**, e37813 (2018).
78. B. Falcon, A. M. Cavallini, R. Angers, S. Glover, T. K. Murray, L. Barnham, S. Jackson, M. J. O'Neill, A. M. Isaacs, M. L. Hutton, P. G. Szekeres, M. Goedert, S. Bose, Conformation determines the seeding potencies of native and recombinant tau aggregates. *J. Biol. Chem.* **290**, 1049–1065 (2015).
79. S. J. Jackson, C. Kerridge, J. Cooper, A. Cavallini, B. Falcon, C. V. Cella, A. Landi, P. G. Szekeres, T. K. Murray, Z. Ahmed, M. Goedert, M. Hutton, M. J. O'Neill, S. Bose, Short fibrils constitute the major species of seed-competent tau in the brains of mice transgenic for human P301S tau. *J. Neurosci.* **36**, 762–772 (2016).
80. J. L. Furman, J. Vaquer-Alicea, C. L. White, N. J. Cairns, P. T. Nelson, M. I. Diamond, Widespread tau seeding activity at early Braak stages. *Acta Neuropathol.* **133**, 91–100 (2017).

81. N. R. Johnson, C. Condello, S. Guan, A. Oehler, J. Becker, M. Gavidia, G. A. Carlson, K. Giles, S. B. Prusiner, Evidence for sortilin modulating regional accumulation of human tau prions in transgenic mice. *Proc. Natl. Acad. Sci. U.S.A.* **114**, E11029–E11036 (2017).
82. C. Xia, S. J. Makaretz, C. Caso, S. McGinnis, S. N. Gomperts, J. Sepulcre, T. Gomez-Isla, B. T. Hyman, A. Schultz, N. Vasdev, K. A. Johnson, B. C. Dickerson, Association of in vivo [$^{18}$F]AV-1451 tau PET imaging results with cortical atrophy and symptoms in typical and atypical Alzheimer disease. *JAMA Neurol.* **74**, 427–436 (2017).
83. C. Condello, P. Yuan, J. Grutzendler, Microglia-mediated neuroprotection, TREM2, and Alzheimer's disease: Evidence from optical imaging. *Biol. Psychiatry* **83**, 377–387 (2018).
84. J. A. Edgeworth, M. Farmer, A. Sicilia, P. Tavares, J. Beck, T. Campbell, J. Lowe, S. Mead, P. Rudge, J. Collinge, G. S. Jackson, Detection of prion infection in variant Creutzfeldt-Jakob disease: A blood-based assay. *Lancet* **377**, 487–493 (2011).
85. L. Concha-Marambio, S. Pritzkow, F. Moda, F. Tagliavini, J. W. Ironside, P. E. Schulz, C. Soto, Detection of prions in blood from patients with variant Creutzfeldt-Jakob disease. *Sci. Transl. Med.* **8**, 370ra183 (2016).
86. M. Bongianni, C. Orrù, B. R. Groveman, L. Sacchetto, M. Fiorini, G. Tonoli, G. Triva, S. Capaldi, S. Testi, S. Ferrari, A. Cagnin, A. Ladogana, A. Poleggi, E. Colaizzo, D. Tiple, L. Vaianella, S. Castriciano, D. Marchioni, A. G. Hughson, D. Imperiale, T. Cattaruzza, G. M. Fabrizi, M. Pocchiari, S. Monaco, B. Caughey, G. Zanusso, Diagnosis of human prion disease using real-time quaking-induced conversion testing of olfactory mucosa and cerebrospinal fluid samples. *JAMA Neurol.* **74**, 155–162 (2017).
87. I. S. Lee, J. R. Long, S. B. Prusiner, J. G. Safar, Selective precipitation of prions by polyoxometalate complexes. *J. Am. Chem. Soc.* **127**, 13802–13803 (2005).
88. D. A. Bennett, A. S. Buchman, P. A. Boyle, L. L. Barnes, R. S. Wilson, J. A. Schneider, Religious orders study and rush memory and aging project. *J. Alzheimers Dis.* **64**, S161–S189 (2018).


**Acknowledgments:** We thank S. Kelley (Abraham Lincoln High School, San Francisco, CA) for assistance with statistical analysis. **Funding:** This work was supported by grants from the National Institutes of Health (NIH) (# AG002132 and AG031220), as well as by the Brockman Foundation, the Dana Foundation, the Glenn Foundation, the Oak Meadow Foundation, the Rainwater Charitable Foundation, and the Sherman Fairchild Foundation. C.C. and W.F.D. are also supported by National Institute on Aging grant (# AG061874). W.F.D. is additionally supported by a National Institute of General Medical Sciences grant (# GM122603). J.S. was supported by the Alzheimer's Association (grant # 2015-NIRG-339935). Human brain tissue was received from the UCSF Neurodegenerative Disease Brain Bank, which is supported by the NIH (# AG023501 and AG19724 to W.W.S.), the Tau Consortium, and the Consortium for Frontotemporal Dementia Research. Human brain tissue was provided by the Brain Bank at Karolinska Institutet (KI), Stockholm, Sweden, which received financial support from StratNeuro at KI, Swedish Brain Power, and Stockholm County Council. Human brain tissue samples also were provided by the Massachusetts Alzheimer's Disease Research Center (director, M. P. Frosch), which received financial support from the NIH (# P50 AG005134). Autopsy brain tissue was obtained from the University of Washington Neuropathology Core, which is supported by the Alzheimer's Disease Research Center (# AG05136), the Adult Changes in Thought Study (# AG006781), and the Morris K. Udall Center of Excellence for Parkinson's Disease Research (# NS062684). C.D.K. is supported by the Nancy and Buster Alvord Endowment. Autopsy brain tissue was also supplied by King's College, University of London (Department of Clinical Neuroscience), the University of Edinburgh (Department of Neuropathology), and the Manchester Brain Bank (University of Manchester), which is part of the Brains for Dementia Research Initiative, jointly funded by the Alzheimer's Society and Alzheimer's Research UK. We thank the Queen Square Brain Bank for Neurological Disorders [supported by the Reta Lila Weston Trust for Medical Research, the Progressive Supranuclear Palsy (Europe) Association, and the Medical Research Council] at the UCL Institute of Neurology, University College London, for provision of the UK human brain tissue samples. The Sydney Brain Bank is supported by Neuroscience Research Australia and the University of New South Wales. G.H. is a National Health and Medical Research Council of Australia Senior Principal Research Fellow (#1079679). Human brain tissue also was provided by the Rush Alzheimer's Disease Center, Rush University Medical Center (director, D. A. Bennett) (*88*), which has received financial support from the NIH (# P30AG10161 and R01AG15819). **Author contributions:** A.A., C.C., J.S., and S.B.P. designed the research. A.A., C.C., J.S., W.Y., B.M.R., and J.C.L. performed the experiments. A.L.W. codeveloped the tauK18(LM)-YFP and α-syn(A53T)-YFP cell lines. G.H., S.v.D., M.I., L.L., C.G., T.D.B., C.D.K., and W.W.S. contributed postmortem human brain samples, generated neuropathology scores, and acquired *APOE* genotypes. A.A., C.C., J.S., W.F.D., and S.B.P. analyzed the data. A.A., C.C., W.F.D., and S.B.P. wrote the paper. C.C. and S.B.P. supervised the study. **Competing interests:** The Institute for Neurodegenerative Diseases (UCSF) has a research collaboration with Daiichi Sankyo (Tokyo, Japan). S.B.P. is the chair of the scientific advisory board of Alzheon Inc. and a member of the scientific advisory board of ViewPoint Therapeutics, neither of which contributed support for this study. W.F.D. is a member of the scientific advisory boards of Alzheon Inc., Pliant, Longevity, Cytegen, Amai, and ADRx Inc., none of which contributed support for this study. W.W.S. received consulting fees from Bristol Myers-Squibb, Merck Inc., and Biogen Idec. A.L.W., A.A., and S.B.P. are coinventors on patent # WO/2017/172764 entitled "Modified cell line and method of determining tauopathies." **Data and materials availability:** All data associated with this study are present in the paper or the Supplementary Materials. All postmortem human brain samples came from tissue banks listed in table S1 and were obtained through material transfer agreements with the indicated institutions associated with the samples.

Submitted 10 April 2018
Accepted 11 January 2019
Published 1 May 2019
10.1126/scitranslmed.aat8462

**Citation:** A. Aoyagi, C. Condello, J. Stöhr, W. Yue, B. M. Rivera, J. C. Lee, A. L. Woerman, G. Halliday, S. van Duinen, M. Ingelsson, L. Lannfelt, C. Graff, T. D. Bird, C. D. Keene, W. W. Seeley, W. F. DeGrado, S. B. Prusiner, Aβ and tau prion-like activities decline with longevity in the Alzheimer's disease human brain. *Sci. Transl. Med.* **11**, eaat8462 (2019).

Science Translational Medicine

# Aβ and tau prion-like activities decline with longevity in the Alzheimer's disease human brain

Atsushi Aoyagi, Carlo Condello, Jan Stöhr, Weizhou Yue, Brianna M. Rivera, Joanne C. Lee, Amanda L. Woerman, Glenda Halliday, Sjoerd van Duinen, Martin Ingelsson, Lars Lannfelt, Caroline Graff, Thomas D. Bird, C. Dirk Keene, William W. Seeley, William F. DeGrado and Stanley B. Prusiner

*Sci Transl Med* **11**, eaat8462.
DOI: 10.1126/scitranslmed.aat8462

**Puncta point the way**

Amyloid plaques composed of Aβ peptides and neurofibrillary tangles composed of aberrant tau proteins are the key pathological hallmarks in the Alzheimer's disease (AD) brain. However, understanding which conformers of Aβ and tau play a pathological role at each step of AD pathogenesis has been difficult to elucidate. Aoyagi *et al.* have developed sensitive cellular assays that detect aberrant Aβ and tau in postmortem brain homogenates from patients with AD or other neurodegenerative diseases. Using fluorescent puncta as a readout, these assays now reveal that patients with AD who died at an older age have lower Aβ and tau pathological conformers than do patients who died at a younger age.